University of Ulm
Institute of Pathology

Head of the Department: Prof. Dr.med. Peter Möller

Influence of different types of amyloid β pathologies on tau pathology in Alzheimer´s disease in different APP-TAU double transgenic mouse models

Doctoral Thesis

for

Medical doctor´s degree

from the

Faculty of medicine

of the

University of Ulm

Silvia Andrea Hipp

Tuttlingen

2017

Officiating Dean: Prof. Dr. rer. nat. Thomas Wirth

First Supervisor: Prof. Dr. Dietmar R. Thal

Second Supervisor: Prof. Dr. Marcus Fändrich

Day of the defence: 13.07.2018

Table of contents

Abbreviations

A	Ampere
Aβ	Amyloid beta
ABC	Avidin biotin peroxidase
AD	Alzheimer´s disease
AMPK	AMP-activated protein kinase
APOE	Apolipoprotein E
APP	Amyloid precursor protein
BSA	Bovine serum albumin
CA	Cornus Ammonis
cDNA	Complementary deoxyribonucleic acid
$C_2H_8O_7H_2O$	Citric acid
$C_6H_5O_7Na_32H_2O$	Sodium citrate
C-terminus	Carboxy-terminus
DAB	Diaminibenzidine
DNA	Deoxyribonucleic acid
ELISA	Enzyme linked inmunosorbent assay
EOAD	early-onset Alzheimer´s disease
FA	Formic acid
FC	Frontocentral cortex
H_2O_2	Hydrogenperoxide
HRP	Horseradish protein
Ig	Immunoglobulin
IP	Immunoprecipitation
KCl	Potassium chloride
kDA	Kilo Dalton
KH_2PO_4	Monopotassium phosphate
LOAD	late-onset Alzheimer´s disease
MAPT	Microtubule-associated protein tau

MARK	Microtubule-associated protein-microtubule affinity regulating kinase
mM	millimolar
MS	Mouse
n	Number of animals
NaCl	Sodium chloride
$Na_2HPO_42H_2O$	Di-sodiumhydrogenphosphate-Dihydrate
NFT	Neurofibrillary tangles
nm	Nanometres
NMDA	N-methyl-D-aspartate
PAR1	Protease-activated receptor 1
PBS	Phosphate buffer saline
PDAPP	Platelet derived APP
PDGF	Platelet derived growth factor-β
PrPc	Cellular prion protein
PSEN1	Persenilin gene 1
PSEN2	Persenilin gene 2
Rb	Rabbit
SDS	Sodium dodecyl sulfate
SDS-PAGE	Sodium dodecyl sulfate polyacrylamide gel electrophoresis
TBS	Tris buffer saline
Thy	Thymocyte
Tris-HCL	Tris hydrochloride
US	United states of America
V	Volt
µg	Microgram
µl	Microliter

1. Introduction

Alzheimer´s disease (AD) is the most common age-related neurodegenerative disorder and the most common cause of dementia in the population older than 65 years of age (Finder 2010). In 2010 4.7 million people at the age of 65 years or older were suffering from AD in the United States of America. If no therapeutic interventions are developed, the number of patients is expected to rise immensely in the next 40 years (Hebert et al. 2013). According to this number of patients, 600.000 people at the age or over 65 years died in 2010 because of AD, representing 32% of all older adults deaths in the US. It is predicted, that this number will rise up to 1.6 million deaths due to AD until 2050 in the US, representing 43% of all older adults deaths (Weuve et al. 2014). These numbers illustrate the impact of Alzheimer´s disease in our society. Thus there is a huge number of people all over the world who will come down with the disease and until today no cure has been found.

Long before clinical symptoms occur, pathological changes in the brain start to develop, up to 20 or more years before the clinical manifestation of AD (Villemagne et al. 2013). In clinically symptomatic stages of the disease the patients show severe loss of cognitive abilities. In the early stages a mild decrease in memory, especially of the short-term memory is the first indicator of the disease. AD, thus, progresses with time to severe dementia. Furthermore, changes of the personality or mood ranging from depressive to aggressive conditions, loss of judgment, orientation and language as well as the decay of elementary physical functions like walking or swallowing, caused by decreased muscle tone occur. Most patients, finally, die in conditions of malnutrition, inanition or pneumonia promoted by bedridden states. In most cases the disease progresses within a timespan of eight to ten years (Bird 2008; Bertram u. Tanzi 2004).

Age itself is regarded as the major risk factor to develop the disease. Actually the incidence of patients increases with age (Bekris et al. 2010). Other risk factors are genetic changes, such as mutations in the APP, Persenilin 1 and Persenilin 2 genes (Bird 2008). Moreover, an association between AD and the apolipoprotein E allele ε4 (APOE ε4) has been found (Strittmatter et al. 1993). The APOE ε4 allele is a risk factor for both, early-onset AD (EOAD) and late-onset AD (LOAD) (see 1.1). In the central nervous system,

apolipoprotein E (apoE) is produced by astrocytes and is involved in the transportation of cholesterol within the central nervous system. Cholesterol as component of cell membranes plays an important role in the formation of new synapses as well as in the repair and plasticity of existing synapses. Apo E4 is less efficient in transporting cholesterol than other isoforms of apoE. Furthermore, it was shown that apoE interacts with the aggregation and clearance of Aβ. It is assumed that Apolipoprotein E4 initiates and accelerates the deposition of Aβ in senile plaques, which is one of the histopathological hallmarks of AD. Also the hyperphosphorylation of tau protein seems to be enhanced by apoE4 (Liu et al. 2013; Strittmatter et al. 1993).

Other risk factors for AD are a family history of AD, alcohol abuse and common cardiovascular risk factors such as obesity, high cholesterol levels and a high systolic blood pressure (Fratiglioni et al. 1993; Kivipelto et al. 2005).

Although AD was first described already in 1907 by Alois Alzheimer, until today the exact mechanisms of the pathogenesis remain unclear. Clinical studies testing potential therapeutic strategies did not show promising results after many years of research and thus no cure is found until today.

This doctoral thesis deals with the pathological mechanisms of AD. First of all, the current knowledge about the pathogenesis of AD is described in the introduction. Then the most important questions for the understanding of the disease are raised, which are still not answered, to then define the aims of this study.

As mentioned above there are several known risk factors for developing AD. Further important risk factors are genetic mutations causing familiar forms of the disease. By means of this, different subtypes of AD can be distinguished.

1.1 Subtypes of Alzheimer´s Disease

On the basis of the age at onset, two different subtypes of AD can be distinguished, early-onset AD (EOAD) and late-onset AD (LOAD). Early-onset AD is characterized by the beginning before the age of 60 to 65 years, representing only 1-6% of all AD cases. About 60% of early-onset AD represent familial forms, whereof 13% are inherited in an autosomal dominant manner (defined as incidence of AD in at least three persons in

three generations) (Campion et al. 1999). Responsible for most of these autosomal dominant inherited forms of AD are mutations in the genes for the amyloid precursor protein (APP), Presenilin 1 and 2 (Bird 2008). Amyloid β protein (Aβ), which is one of the major players in AD´s pathology (see 1.2 and 1.3), is produced by the cleavage of APP. Mutations in the APP gene leading to an overproduction of Aβ can hence cause familial forms of AD. The genes for Presenilin 1 and 2 encode for transmembrane proteins, which are part of the γ-secretase. This is the enzyme, which generates Aβ by cleaving its precursor protein, APP (Bekris et al. 2010).

LOAD is defined as the onset after the age of 60 to 65 years (Bekris et al. 2010). For LOAD there is no inheritance following Mendel´s laws. The main genetic risk factor for this subtype of AD is the presence of one or two copies of the APOE ε4 allele (Bird 2008; Breitner et al. 1999).

1.2 Pathological features of Alzheimer´s Disease

Although the pathomechanism of AD is not yet fully understood, typical pathological changes are known. Already in 1907, Alois Alzheimer described the main histopathological findings seen in AD brains.

These are extracellular deposits of the amyloid β protein (Aβ) (Masters et al. 1985) and thickened neurofibrillary structures, consisting of intracellular aggregates of abnormally phosphorylated tau protein, forming neurofibrillary tangles (NFT) (Grundke-Iqbal et al. 1986). In AD, the extracellular depositions of Aβ present as senile plaques (Masters et al. 1985).

Alzheimer himself already saw that these changes lead to a reduction of neurons and a reactive gliosis in the brain. These microscopic changes were associated with macroscopically visible atrophy of the brain (Alzheimer A. 1907; Double et al. 1996). This atrophy affects mainly the cortical and subcortical areas and is 20-25% greater than in age-related healthy people´s brains (Double et al. 1996). Another major finding in AD is the loss of synapses, being the major correlate for cognitive impairment (Terry et al. 1991).

These neuropathological findings are hallmarks of the disease and also serve as diagnostic criteria. Being certainly diagnosed only by histological analyses of the brain, the definite diagnosis of AD is possible only postmortem (Finder 2010).

1.3 Amyloid precursor protein (APP)

As mentioned above, deposits of amyloid β protein are one typical feature of AD. Aβ is a protein which is generated by the proteolytic cleavage APP. The 400kb gene for APP is located on the long arm of chromosome 21 at position 21, consisting of at least 18 exons (Lamb et al. 1993; Kang et al. 1987). By alternative splicing, three different isoforms of APP may arise: APP695, APP751 and APP770, differing in their amount of amino acids (Tanaka et al. 1988).

APP is a transmembrane protein; its hydrophilic amino acid terminus reaches into the extracellular space, whereas the short C-terminus lies within the cytosol (Kang et al. 1987; Haass et al. 2012).

The physiological functions of APP are not fully understood, although it resembles a cell-surface receptor, no ligand has been identified yet (Kang et al. 1987; Rice et al. 2013). Interactions of APP with components of the extracellular matrix like heparin, laminin and collagen were observed, leading to the assumption that APP might play a role in cellular adhesion (Clarris et al. 1997, Kibbey et al. 1993, Beher et al. 1996).

1.4 Amyloid-beta

Aβ is generated by proteolytic cleavage of APP. For APP cleavage two different pathways can be distinguished; an amyloidogenic and a non-amyloidogenic pathway.

In the non-amyloidogenic pathway, APP is cleaved by a protease called α-secretase. The cleavage site of this enzyme is located within the Aβ-domain of APP (De Strooper et al. 2010). Therefore, no functional Aβ-peptide is produced via α-secretase cleavage. A soluble APPsα fragment is released from the membrane-bound carboxy-terminal portion

(De Strooper et al. 2010); the fragment remaining in the membrane is either degraded via lysosomes or further cleaved by γ-secretases (De Strooper et al. 2010).
In the amyloidogenic pathway, APP cleavage starts with the β-secretase. This enzyme reaches its optimum activity in a low pH environment and is manly found in intracellular compartments like the trans-Golgi system or endosomes providing an acid milieu (De Strooper et al. 2010). The β-secretase cleaves APP at its extracellular lying portion generating a molecule called APPsβ, which is released into the extracellular space. The carboxy-terminal fragment remaining in the membrane undergoes further cleavage by γ-secretase, which finally leads to the release of the Aβ peptide. The functional Aβ-peptide is released into the extracellular room, where it is able to aggregate, to oligomerize and finally to deposit in senile plaques. As the cleavage site of γ-secretase is not exact, the generated Aβ peptides may slightly differ in the amount of amino acids with most of them being 40 amino acids long (Vassar 2001; Haass et al. 2012).
If an overproduction of Aβ occurs (like in familial forms of AD) or if there is a dysfunction of the clearance of Aβ, the peptides can accumulate, aggregate and, finally, deposit in plaques. Known ways of Aβ clearance are the transport over the blood-brain barrier or the enzymatic degradation via peptidases such as neprilysin and insulin-degrading enzyme (Wang et al. 2006).

Amyloid-β plaques

Aβ can aggregate and accumulate in plaques, which is one of the hallmarks of AD. Therefore, some characteristics of Aβ plaques in AD shall be illustrated.
The term “senile plaque” summarizes all kinds of deposits of Aβ in the brain, which are non-vascular. These plaques may also occur in healthy people´s brains but the distribution through the brain differs from patients suffering from AD. In non-demented people the Aβ plaques can be found mainly in the cortical brain regions, the thalamus and the basal ganglia. In AD patients the plaques also arise in deeper brain regions like the brain-stem, mid-brain and the cerebellum as well (Thal et al. 2006; Price et al. 1991).
For AD, a hierarchical sequence of Aβ deposition has been described. The Aβ deposits first arise in frontal, parietal, temporal and/or occipital neocortical areas. In the next phase

further deposits occur in the entorhinal CA1 region and/or the insular cortex, followed by subcortical areas, brainstem nuclei and the cerebellum (Thal et al. 2002).
The three dimensional structure of proteins is essential for their physiological function. Misfolded proteins are normally removed quickly. It is assumed that the aggregation of such proteins leads to neurodegenerative diseases such as AD or for example Huntington's disease or amyotrophic lateral sclerosis. The term "amyloid" was originally used for extracellular aggregations of proteins organized in a cross-β structure, which characteristically bind to Congo red and thioflavin S (Soto 2003). For the aggregation it is supposed that a core protein is necessary, which acts as a seeding point from which further aggregation arises (Soto 2003).

Aβ-Toxicity

Although the exact pathological mechanisms in AD are not yet completely understood, several in vitro and in vivo studies showed that soluble oligomeric Aβ is able to cause a decrease in synaptic plasticity as well as a decrease in long-term potentiation in neurons (Townsend et al. 2006; Cleary et al. 2005; Billings et al. 2005). Such changes could lead to decreased cognitive abilities in AD´s patients.
Furthermore, Aβ might cause damages in neuronal mitochondria and decrease mitochondrial motility, which leads to disorganized mitochondria at the synapses. Especially, the synaptic mitochondria play an important role for a proper function of the synapses (Du et al. 2012).
Other studies show that Aβ interferes in calcium signaling in neurons. This is also a possible way how Aβ might cause neurodegeneration (Demuro et al. 2010) leading to cognitive decline.

1.5 Tau protein

Tau protein is known to be a microtubule stabilizing protein and is mainly localized in the axon of a neuron. The tau-gene is located on chromosome 17. Tau is expressed most

notably in neurons; this could be due to interactions with a specific neuronal factor or because of eventually existing silencer molecules in non-neuronal cells.
Tau-protein supports the assembly of tubulin, leading to the stabilization of microtubules. Microtubules are part of the cytoskeleton, which stabilize the cell. Furthermore, microtubules serve as a leading structure for motor proteins like dynein and kinesin. Therefore, tau protein is able to influence axonal transport in the neuron (Ebneth et al. 1998).
In human brains six different isoforms of tau are found, which are generated by alternative splicing, differing by the number of 29-residue near-amino-terminal inserts (Avila et al. 2004). Moreover, tau protein seems to have a DNA protective function. By binding to DNA it increases the DNA´s melting temperature and, thereby, protects the integrity of the DNA (Camero et al. 2014). It was shown that tau accumulates in the nucleus under conditions of oxidative stress, protecting the integrity of the DNA (Violet et al. 2014).
The molecular structure of the tau protein can be divided into two different domains: the amino-terminal end containing the projection domain, and the microtubule binding domain, consisting of the carboxy terminal part of the molecule (Wang u. Mandelkow 2016).
The projection domain plays different roles in the neuron. On the one hand, it is responsible for the spacing of microtubules in the axon (Chen et al. 1992); on the other hand, it might play a role in the subcellular distribution of tau (Liu u. Gotz 2013). Natural tau protein is normally unfolded and shows only little tendency for aggregation.

Phosphorylation of tau

Phosphorylation of tau also occurs to a certain degree in healthy conditions. The extent of phosphorylated tau decreases during the brain development. Fetal tau shows a higher degree of phosphorylation than normal adult tau, which carries approximately two phosphates (Kanemaru et al. 1992). In AD the phosphorylation is further increased to approximately eight phosphates per molecule. In the longest isoform of tau there are about 85 sites where phosphorylation is possible (Wang u. Mandelkow 2016).

Phosphorylation of tau at different sites can have different effects. For example it can reduce the affinity of tau to microtubules and hence lead to a detachment of tau from the microtubules (Hanger et al. 2009) . Furthermore, hyperphosphorylation might trigger missorting of tau from the axons to the perikaryon, leading to synaptic dysfunction, possibly because of impaired trafficking of receptors (Hoover et al. 2010).

Aggregation of tau

As tau is normally unfolded, it shows only little tendency to aggregate. Nevertheless aggregation of tau protein is characteristic for several neurodegenerative diseases known as tauopathies. It is thought that aggregation of tau is promoted by its hyperphosphorylation (Braak et al. 1994) and that the aggregation might indirectly be triggered by hyperphosphorylation through the resulting detachment of tau from microtubules (Wang u. Mandelkow 2012). Furthermore, it is not yet clear whether there are still unknown cofactors to play a role in tau aggregation.

Loss of tau function

As a result of tau hyperphosphorylation and aggregation the level of functional tau in the brain decreases, which leads to a detachment of tau from microtubules. This might cause a breakdown of the axonal transport systems of the neuron. As mentioned earlier tau also plays a role in DNA protection. Probably, the loss of these physiological functions of tau may contribute to neurodegeneration.

1.6 Amyloid-cascade-hypothesis

With the discovery of Aβ as the main component of AD plaques in 1985, the first ideas came up that Aβ might trigger the pathological changes seen in AD (Masters et al. 1985). Eight years later, the amyloid-cascade-hypothesis was postulated, proposing that the typical histopathological changes seen in AD are result of progressive Aβ-aggregates (Hardy u. Higgins 1992). Crucial for the formulation of this hypothesis was the fact that

the APP gene is located on chromosome 21, explaining why people with Down´s syndrome develop typical AD pathology. Furthermore, it was known that mutations found in the APP can cause AD (Scheuner et al. 1996), whereas mutations in the tau gene caused a specific type of frontotemporal dementia (Hutton et al. 1998). Although a lot of findings support the amyloid-cascade-hypothesis it is not yet proven and has undergone several modifications during the time (Selkoe 2011; Selkoe u. Hardy 2016). Nevertheless, it is widely accepted that Aβ plays a crucial role in AD pathogenesis and the amyloid-cascade-hypothesis has become to the most influent hypothesis in the field of AD research. But until today it is not fully clear whether intra- or/and extracellular localized Aβ influences tau pathology. It has already been shown, that Aβ is able to aggravate tau pathology in tau transgenic animal models (Gotz et al. 2001; Lewis et al. 2001; Oddo et al. 2004), but we do not yet understand how.
The interrelationships between tau-pathology and extra- or intracellular located Aβ shall be analyzed in my project using transgenic mice, which serve as animal models for tau and different types of Aβ pathology.

1.7 Transgenic mouse models of AD

To clarify the pathogenesis of AD experimental mouse models have been developed. The mouse models have become very important tools for research to understand the pathological mechanisms of the disease. Furthermore, they have been used to test potential disease modifying therapies.
There are three different genes, in which mutations can cause autosomal dominant inherited forms of AD; these are APP and the persenilin genes (PSEN1 and PSEN2) (Brunkan u. Goate 2005). The overexpression of these AD-associated genes in mice was and is the fundament for most mouse models expressing Aβ pathology. Mutations in the MAPT gene, which are responsible for causing different non-AD tauopathies, such as frontotemporal dementia (Hutton et al. 1998) are the basis for mouse models developing tau pathology (Hutton et al. 2001).
To overexpress transgenes in mouse models different promoters are used.

PDAPP mice

Platelet-derived growth factor-β (PDGF) promoter, which is known to be highly expressed in the central nervous system, was used for a mouse model carrying the APPV717F familial AD mutation. These mice are called PDAPP mice, which is a term combining the PDGF promoter and APP. The mice show a 10-fold elevation of human APP protein compared to mouse protein (Elder et al. 2010). PDAPP mice develop age-dependent Aβ deposits including dense core plaques in the hippocampus and cerebral cortex similar to those seen in humans. Furthermore, reactive astrocytes, activated microglia and dystrophic neurons can be found in association with the plaques. Plaque deposition, thereby, starts with 6 months of age and increases to very high levels at the age of 12 to 15 months (Games et al. 1995; Reilly et al. 2003).

Tg2576 mice

Another mouse model based on a mutation in the APP gene is the Tg2576 mouse. These animals overexpress a human transgene APP with the Swedish familial AD Mutation (K670N/M671L) (the mutations are named after the geographical region the affected family comes from) driven by a hamster prion promoter. This promoter drives a very strong expression but is less selective than others as it also expresses the transgene in glia and in extraneuronal tissues (Hall u. Roberson 2012). The Tg2576 mice also develop parenchymal Aβ plaques at the age of 11 to 13 months, which come along with gliosis and dystrophic neurites. Also develop vascular deposits of Aβ are seen (Hsiao et al. 1996; Elder et al. 2010).

APP23 mice

APP 23 mice overexpress a 751 amino acid isoform of mutated human APP seven-fold, harboring the Swedish mutation under control of a Thy-1-promoter (Sturchler-Pierrat et al. 1997). This promoter allows elevated and selective expression of APP in neuronal cells. In consequence, these animals show progressive extracellular aggregates of Aβ. The first plaques occur at the age of six months in the neocortex and hippocampus, increasing in

number and size with the age (Sturchler-Pierrat et al. 1997). Inflammatory changes, i.e. microglial reactions associated with reactive astrocytes can be found in the areas around the plaques (Sturchler-Pierrat et al. 1997). Additional, neuritic and cholinergic dystrophy occur (Sturchler-Pierrat et al. 1997). In the distorted neurites which are surrounding the plaques hyperphosphorylated tau protein can be found in mice at the age of 12 months and older (Sturchler-Pierrat et al. 1997). Aβ-generation in these mice follows the β- and γ-secretase pathways. In contrast to PDAPP and Tg2576 mice, the APP23 mice show neuronal death in the hippocampal CA1 region (Calhoun et al. 1998). Therefore, the APP23 mouse is the only APP single transgenic mouse model which shows AD-typical neuronal cell loss by overexpressing only APP.

APP51/16 mice

APP51/16 mice overexpress human wild-type APP under the control of a Thy-1-promoter (Herzig et al. 2004; Thal et al. 2009). These animals also show extracellular Aβ-plaques but in contrast to the APP23 mice they do not develop neurodegeneration and show less severe Aβ accumulation and plaque pathology beginning with 11 months of age (Rijal Upadhaya et al. 2012). No NFT are found. Aβ in these animals is mainly generated by the endosomal pathway by β- and γ-secretases cleavage. α-secretase cleavage of APP, representing the non-amyloidogenic pathway occurs in the APP51/16 mice more predominant than in APP23 mice (Rijal Upadhaya et al. 2012).

APP48 mice

In APP48 mice the cDNA encoding the 42 amino acid isoform of human Aβ has been linked to a rat proenkephalin signal peptide. This leads to insertion of the Aβ peptide into the endoplasmic reticulum (Abramowski et al. 2012). In so doing, this mouse model exhibits the synthesis of Aβ in the endoplasmic reticulum. These animals do neither show extracellular Aβ-plaques at any age nor neurons accumulating abnormally phosphorylated tau protein (Abramowski et al. 2012). The APP48 mice show only intracellular deposits of Aβ (Abramowski et al. 2012).

TAU58/2 mice

The TAU58/2 mice carry the P301S mutation for the 363 amino acid isoform of human four-repeat tau protein under the control of a murine Thy-1-promoter (van Eersel et al. 2015). Already at the age of 3 months occasional Gallyas-positive neurofibrillary tangles are found in the frontocentral cortex but more frequently in the brainstem. The number of neurofibrillary tangles increases with age. At the age of one month the mice already present with lower bodyweights compared to normal animals. Motor deficits and coordination problems are seen at the age of 6 months (van Eersel et al. 2015).

The aim of this study is to find out more about the interactions between Aβ and tau. Therefore, doubletransgenic mouse models shall be examined. I chose to cross APP23, APP51/16 and APP48 mice with TAU58/2 transgenic mice, to see the interplay between Aβ and tau when they are produced endogenously at the same time in the mouse brain. APP23 mice are selected as these are the only APP transgenic mice presenting with loss of neurons.

APP51/16 mice are constructed in the same way as APP23 mice are, with the difference that they do not harbour mutant APP, but they overexpress human wildtype APP. As they produce less Aβ than the APP23 mice, the effects of the presence of more or less Aβ can be compared.

APP48 mice provide the possibility to examine the effects of intracellular Aβ on tau pathology. Although it is a very artificial model of Aβ pathology it provides the opportunity to see effects of Aβ pathology, which cannot be seen under physiological circumstances. Furthermore, the effects of Aβ can be studied, when it is generated independent from APP cleavage.

TAU58/2 mice serve as model for tau pathology in this study. The animals develop distinctive tau pathology already at young ages.

The selected crossbred mouse models have not yet been examined before.

1.8 Interactions between Aβ and tau

Aβ and tau, the main components of the histopathological hallmarks in AD are in the focus of AD research. In the last years an increasing interest is directed towards possible interactions between the two proteins. Studies have revealed that there has to be a link between Aβ and tau in the pathomechanism of AD. Although the exact molecular mechanism of this interaction remains unclear, progress in the understanding was made. The interplay between Aβ and tau at the synapses is of special interest, because loss of synapses is one important finding in AD and it represents the histological correlate for cognitive decline in AD patients. Furthermore, the synapses may represent an important point of interaction where extracellular Aβ and intracellular tau get in touch.

Aβ is known to influence postsynaptic NMDA receptors, although it is not yet clear whether Aβ directly binds to the receptor or if it influences them indirectly via interaction with membrane structures or membrane receptors. It is assumed that Aβ causes excitotoxicity due to an over-excitation of NMDA receptors and hence causes spine loss (Roberson et al. 2007; Ittner u. Gotz 2011). Moreover, Aβ down regulates the number of NMDA receptors and enhances their internalization. A loss of postsynaptic NMDA receptors finally leads to a decreased calcium influx into dendritic spines, causing shrinkage and retraction of synaptic spines (Shankar et al. 2007; Snyder et al. 2005).

We further know that Aβ binds to the cellular prion protein (PrPc), a protein which acts as a cell surface receptor. This induces the activation of Rrc kinase Fyn, which ultimately leads to phosphorylation of NMDA receptors and hence a loss of surface NMDA receptors (Um et al. 2012).

Tau also interacts with Fyn; under physiological conditions it targets Fyn to the spine. At the spine, Fyn phosphorylates NMDA receptors which causes excitotoxicity (as mentioned earlier) and the loss of NMDA receptors (Ittner et al. 2010). If Aβ and hyperphosphorylated tau occur in increased levels more Fyn is targeted to the dendritic spines. In so doing, tau acts synergistic with the toxic effects of Aβ on NMDA receptors. Aβ initially leads to over excitation of NMDA receptors and hence to an elevated localized calcium influx into the cell (Zempel et al. 2010). The increased calcium levels activate the kinases AMPK and PAR-1/MARK which cause tau phosphorylation (Mairet-Coello et al. 2013). Furthermore, it has been proposed that Aβ might activate Fyn and hence

accelerates loss of synapses (Yu et al. 2012; Mairet-Coello et al. 2013). These findings show different ways how Aβ and tau both interact with synaptic receptors and hence also interact with one another. Aβ can trigger the phosphorylisation of tau via the activation of AMP and PAR-1/MARK kinases and tau itself aggravates the toxic effects of Aβ via targeting Fyn. Taken together, there is evidence that rising levels of Aβ lead to rising tau pathology in form of NFT formation and vice versa (Spires-Jones et al. 2017).

1.9 Aims of the study

The overall aim of this study is to get a further insight into the interactions between Aβ and tau and its effects on the development of pathological lesions: neurofibrillary tangles and senile plaques. To address this overall aim, different APP and tau double transgenic mice that vary in the amount and manner of Aβ production will be examined to test and compare the interplay between Aβ and tau under different conditions. This will allow clarifying whether seeding and perhaps cross-seeding of Aβ and tau occurs and under which conditions such interactions can be seen. The results of these experiments help to get a better understanding of the pathological mechanisms in AD and so, perhaps help to find novel therapeutic strategies for the treatment of AD.

2. Material and Methods

Table 1: Buffers, reagents and antibodies used for immunohistochemical staining and Western blot analysis

A) Tris buffer saline (TBS)

Name	Amount/concentration	Source
Tris-HCL	20 mM	Merck, Darmstadt, Germany
NaCl	150 mM	Merck, Darmstadt, Germany
Destilled water	To 1 liter	Millipore GmbH, Schwalbach, Germany

B) Phosphate buffer saline (PBS)

KCl	2,7 mM	Merck, Darmstadt, Germany
KH_2PO_4	1,46 mM	Merck, Darmstadt, Germany
NaCl	137 mM	Merck, Darmstadt, Germany
$Na_2HPO_42H_2O$	8,1 mM	Merck, Darmstadt, Germany
Destilled Water	To 1 liter	Millipore GmbH, Schwalbach, Germany
Tween (for PBS-T)	0,05%	Bio-Rad, CA, USA

C) Citrate buffer

$C_6H_8O_7H_2O$	0,1 M	Merck, Darmstadt, Germany
$C_6H_5O_7Na_32H_2O$	0,1 M	Merck, Darmstadt, Germany

D) Further reagents used for immunohistochemical staining

3,3'-Diaminobenzidine (DAB)	Merck, Darmstadt, Germany
Ethanol	Sigma-Aldrich, Steinheim, Germany
Formic acid	Applichem, Darmstadt, Germany
Hydrogen peroxide	Fischar, Saarbrücken, Germany
Xylene	Merck, Darmstadt, Germany

E) Blocking buffer:

Triton X	0,25 g	Sigma Taufkirchen, Germany
DL-Lysin	1,82 g	Sigma Taufkirchen, Germany
BSA	10 g	Sigma Taufkirchen, Germany
TBS	100 ml	See above

F) ABC (Detector Complex):

TBS	10 ml	See above
Reagent A	150 µl	ABC-Kit, Vector Laboratories, CA, USA
Reagent B	150 µl	ABC-Kit, Vector Laboratories, CA, USA

G) Blocking antibody (for AT 8 immunohistochemical staining):

Anti-Mouse IgG (Fragment)	Biomeda, CA, USA,

H) Primary antibodies:

	Antigen	**Species**	**Dilution**	**Pre-treatment**	**Source**
AT8	Abnormally phosphor-ylated tau protein	MS-Monoclonal	1:1000; 1:100 for immunofluorescence double staining	Microwave and formic acid	Pierce Thermo Scientific, MA, USA
RD 3	3-repeat Tau	MS-Monoclonal	1:500	Microwave and formic acid	Millipore GmbH, Schwalbach, Germany
RD 4	4-repeat Tau	MS-Monoclonal	1:1000	Microwave and formic acid	Millipore GmbH, Schwalbach, Germany
Anti Aβ40	Aβ32-40	Rb-Polyoclonal	1:100	Formic acid	IBL, Minneapolis, USA
Anti Aβ42	Aβ1-42	Rb-Polyoclonal	1:100	Formic acid	IBL, Minneapolis, USA
4G8	Aβ17-24	MS-Monoclonal	1:1000	Formic Acid	Covance, Dedham, USA
6E10	Amyloid β 1-17	MS-Monoclonal	1:1000		Anti-MS-HRP, Bio-Rad

I) Secondary antibodies:

	Type	Concentration/dilution	Source
	Biotin anti-Mouse	10 ml Tris + 50 µl Biotin secondary antibody	ABC kit, Linaris, Wertheim, Germany
	Biotin anti-Rabbit	10 ml Tris + 50 µl Biotin secondary antibody	ABC kit, Linaris, Wertheim, Germany
Cy2	Anti-Mouse IgG (for immunofluorescence double labelling)	1:50	Jackson Immunoresearch Labs Inc., West Baltimore, USA
Cy3	Anti-Rabbit IgG (for immunofluorescence double labelling)	1:50	Jackson Immunoresearch Labs Inc, West Baltimore, USA

Table 2: Reagents used for Gallyas staining

A) Alkaline silver iodide solution

Name	Amount/concentration	Source
Potassium Iodide	10g	Merck-Schuchardt, Hohenbrunn, Germany
1% Silver nitrate	3,5ml	Merck-Schuchardt, Hohenbrunn, Germany
Destilled water	50ml	Millipore GmbH, Schwalbach, Germany

B) Developer solution

Sodium carbonate	50g	Merck-Schuchardt, Hohenbrunn, Germany
Ammonium nitrate	2g	Merck-Schuchardt, Hohenbrunn, Germany
Silver nitrate	2g	Merck-Schuchardt, Hohenbrunn, Germany
Tungstosilicic acid	10g	Merck-Schuchardt, Hohenbrunn, Germany
Destilled water	1000ml	Millipore GmbH, Schwalbach, Germany
35% Formaldehyde		

C) Further reagents used for Gallyas staining

5% Periodic Acid	Merck-Schuchardt, Hohenbrunn, Germany
0.5% Acetic Acid	Merck-Schuchardt, Hohenbrunn, Germany
1% Sodium thiosulphate	Merck-Schuchardt, Hohenbrunn, Germany
0.1% Gold Chloride	Merck-Schuchardt, Hohenbrunn, Germany

Table 3: Kit used for immunoprecipitation

µMACS Protein G MicroBeads	Miltenyi Biotec, Bergisch Gladbach, Germany
µMACS separation columns	Miltenyi Biotec, Bergisch Gladbach, Germany

Table 4: Kit used for detection and quantitation of total protein

Pierce® BCA Protein Assay Kit	Pierce Biotechnology, Rockford, USA

Table 5: Used ELISA Assay kit

MSD® MULTI-SPOT Phospho (Thr231)/ Total Tau Assay	Meso Scale Discovery, Rockville, USA

Table 6: Centrifuges, Microscopes and other technical equipment

Centrifuges		
Cool centrifuge	Centrifuge 5417R Rotor F-45-30-11	Eppendorf, Hamburg, Germany
Speedvac centrifuge	Concentrator 5301	Eppendorf, Hamburg, Germany
Table centrifuge	Mikro 200	Hettich Zentrifugen, Tuttlingen, Germany
Ultracentrifuge	Optima MAX-E	Beckmann Coulter, Krefeld, Germany
Magnetic stand for IP	µMACS	Miltenyi Biotech,Bergisch Gladbach, Germany
Magnetic stirrer	MR Hei Standard	Heidolph Instruments, Solingen, Germany
Microscopes		
	Fluorescence Microscope Leica DMLB	Miltenyi Biotech, Bergisch Gladbach, Germany
	Scanning Confocal Microscope Leica TSC NT	Leica, Bersheim, Germany
Protein blotting	Criterion Blotter	Bio-Rad, CA, USA
Protein Gel electrophoresis chamber	XCell4 SureLock™ Midi-Cell	Invitrogen, CA, USA
Roller Mixer	Stuart SRT6	Bibby Scientific, Staffordshire, UK
Shaker	SM-30	Edmund Bühler GmbH, Hechingen, Germany
Sonicator	SONOPLUS HD 2070	Bandelin electronic, Berlin, Germany
Thermomixer	Thermomixer 5436	Eppendorf, Hamburg, Germany
Vortex	VM 3000 Mini vortexer	Henry Troemner LLC, NJ, USA

Table 7: Used Software

Corel Photo Paint 12	CorelDRAW, Unterschleissheim, Germany
IBM SPSS Statistics 21 and 24	Chicago, IL, USA
Image J	NIH, Bethesda, MD, USA
KC4 V3.1	Bio-Tek Instruments, Inc., Winooski, VT, USA
Leica FireCam Software	Leica, Bersheim, Germany
Leica TCS Software	Leica, Bersheim, Germany
Microsoft Office	Microsoft, CA, USA
Windows XP	Microsoft, CA, USA
Windows Vista	Microsoft, CA, USA
Windows 10	Microsoft, CA, USA
RefWorks	ProQuest, Michigan, USA

2.1 Animals

All animals were sacrificed and tissue samples were provided as a gift by the Novartis Institutes for Biomedical Research (Basel, Switzerland) for biochemical and histological studies.

Generation of APP23 mice was performed as previously described (Sturchler-Pierrat et al. 1997) and continuously back-crossed to C57BL/6. To drive neuron-specific overexpression of human APP751 harbouring the Swedish double mutation 670/671 KM→NL, a murine Thy-1 cassette was used as promoter.

Also APP51/16 mice were generated as described previously (Herzig et al. 2004) and continuously back-crossed to C57BL/6. Like in APP23 mice, also a murine Thy-1 promoter was used to drive neuron-specific expression, with the difference that APP51/16 mice express human wild-type APP instead of mutant APP.

APP48 mice were bread as described previously (Abramowski et al. 2012), they were also continuously back-crossed to C57BL/6. For APP48 mice again a murine Thy-1 expression cassette was used to drive neuron-specific expression of the rat proenkephalin signal sequence followed by human wild type Aβ1-42 to drive neuron-specific expression of human wild type Aβ1-42.

Each of the APP transgenic mouse models was crossbred with TAU58/2 mice carrying the P301S mutation for the 363 amino acid isoform of human four-repeat tau protein under the control of a murine Thy-1-promoter. TAU58/2 mice were generated as described previously (van Eersel et al. 2015). The animals were crossbred and sacrificed at 6 months of age; no other experiments were performed with them.

TAU 58/2 mice and APP single transgenic mice serve as control group.

All animal crossbreeding experiments as well as mouse euthanasia were performed at the Novartis Institutes for Biomedical Research in Basel (Switzerland). Animals were treated in agreement with the Swiss law for the use of laboratory animals. The permission for the experiments was granted by the Kantonales Veterinäramt Basel-Stadt (BS-1795, BW-1094, BW-444). For euthanasia, the animals were anaesthetized with isoflurane and then decapitated. The mouse brains were removed and either embedded in paraffin or the forebrains were homogenised and stored at -80 °C. For homogenisation, the forebrains were weighed and diluted with homogenization buffer TBS-Complete and PhosStop

Protease inhibitor cocktail tablets (Roche, Switzerland) to the final dilution 1:10, followed by sonication. We received tissue samples of these mice governed by a material transfer agreement between the Novartis pharma AG (Basel, Switzerland) and the University of Ulm for biochemical and microscopic analysis. The number of animals examined by immunohistochemical staining, western blotting and ELISA analyses is shown in table 8, 9 and 10.

Table 8: Mice examined by immunohistochemistry

Genotype	Number of mice	Male	Female	Age
APP23xTAU58/2	10	5	5	6 months
APP48xTAU58/2	10	3	7	6 months
APP51xTAU58/2	8	4	4	6 months
TAU58/2	18	8	10	6 months

Table 9: Mice examined by Western blotting

Genotype	Number of mice	Male	Female	Age
APP23xTAU58/2	6	3	3	6 months
APP51/16xTAU58/2	6	3	3	6 months
APP48xTAU58/2	6	3	3	6 months
TAU58/2	6	3	3	6 months

Table 10: Mice examined by Phospho tau and total tau ELISA

Genotype	Number of mice	Male	Female	Age
APP23xTAU58/2	4	2	2	6 months
APP51/16xTAU58/2	6	3	3	6 months
APP48xTAU58/2	6	2	4	6 months
TAU58/2	6	3	3	6 months
APP23	2	1	1	6 months
APP51/16	2	1	1	6 months
APP48	2	1	1	6 months

2.2 Immunohistochemistry

For detection of hyperphosphorylated tau-protein AT8, a monoclonal mouse antibody was used. RD3 and RD4 monoclonal antibodies were used to detect three- (RD3) and four-repeat (RD4) tau, respectively. A polyclonal rabbit antibody, Aβ42 was used to detect Aβ1-42. Ten APP23xTAU58/2, ten APP48xTAU58/2, eight APP51xTAU58/2 and eighteen TAU58/2 mice were analyzed (see table 8). For immunofluorescence double staining two APP23xTAU58/2, two APP48xTAU58/2 and one APP51/16xTAU58/2 mice were examined. For this purpose, AT8 and 4G8 antibodies were used for APP23xTAU58/2 and APP51/16xTAU58/2 mice to detect hyperphosphorylated tau protein and Aβ. In APP48xTAU58/2 mice Aβ was detected with anti Aβ42 antibody, binding to Aβ1-42.

Deparaffinization

For immunohistochemical staining of paraffin sections, paraffin was removed by treatment with xylene, three times for five minutes, and then, sections were hydrated in a sequence of descending concentrations of ethanol. In detail, the sections were dipped in ethanol 100%, followed by resting in ethanol 100% for five minutes, followed by five minutes in ethanol 96% and five minutes in ethanol 70%. After washing the sections with destilled water, they were incubated in a mixture of 200 ml destilled water, 25 ml hydrogen peroxide and 25 ml methanol for thirty minutes, to block the endogenic peroxidases. Two washing steps in destilled water followed.

Microwave and formic acid pretreatment

For antigen retrieval the sections were pre-treated in the microwave and with formic acid (for staining with AT8, RD3 and RD4). For staining with Aβ42 and 4G8 antibody pre-treatment with formic acid was performed.
For microwave pre-treatment the brain sections incubated in 10 mM citrate buffer (pH 6. 0) for 15 minutes in the microwave oven at maximum temperature. After cooling of the sections they were washed in Tris buffer (pH 7.4).

For the formic acid pre-treatment, brain sections were incubated in formic acid for three minutes, followed by a washing step with Tris buffer.

Blocking antibody

To prevent unspecific binding of the secondary antibodies to intrinsic mouse IgG, we used 10% human bovine albumin. A goat-derived anti-mouse IgG antibody was used to block detection of intrinsic mouse IgG. The blocking antibody was incubated in a wet chamber overnight at room temperature (this step was not necessary for staining with anti Aβ40 and anti Aβ42 antibody, because these are rabbit derived antibodies, detected with anti-rabbit IgG secondary antibody).

Primary antibody

After washing the sections in Tris buffer, they were incubated with the primary antibody overnight at room temperature.

Secondary antibody

After another washing step in Tris buffer at pH 7.4, the secondary biotinated antibodies were incubated on the sections for 90 minutes (for staining with AT8, RD3, RD4, anti Aβ40 and anti Aβ42). The secondary antibodies used for immunofluorescence double labelling, Cy2-labelled anti-mouse IgG and Cy3-labelled anti-rabbit IgG (dilution 1:50) were incubated for two hours on the sections in the dark in a wet chamber. Then again, the sections were washed in Tris buffer at pH 7.4.

Signal amplification and counterstaining

To amplify the signal of the biotin antibodies, ABC detector complex was used for staining with AT8, RD3, RD4 and anti Aβ40 and 42 antibodies, which incubated for 120 minutes in a wet chamber. DAB was used as chromogen inducing a brown staining. For counterstaining hemalum was used.

Dehydratization and mounting of the sections

Dehydrogenation in a sequence of ascending concentrations of ethanol and in xylene followed (reversed order as used for hydratization of the sections). Finally, the sections were mounted in Eukitt (O. Kindler; Freiburg, Germany).
For immunofluorescence double labelling, the sections were washed in Tris buffer after incubation of the secondary antibody. After washing in destilled water, the section dried at 30°C for 30 minutes. Thereafter, the sections were incubated in xylene for 2 seconds and mounted in Eukitt (O. Kindler; Freiburg, Germany).

2.3 Gallyas staining

For Gallyas staining the sections were placed in alkaline silver iodide solution for 1 minute. Then they were washed in 0.5% acetic acid three times for one minute and the sections were placed into the developer solution (see table 2) for about 5-30 minutes, until a light grey or brown staining was noticed. After another washing step in 0.5% acetic acid the sections were incubated in 1% sodium thiosulphate solution for 5 minutes. After washing with destilled water the sections were placed in 0.1% gold chloride for 5 minutes. Another washing step with destilled water followed before the sections were placed in an 1% sodium thiosulphate solution for five minutes as a last step before mounting the sections in Eukitt.

2.4 Number of neurons affected by abnormal phosphorylated tau-protein

The percentage of AT8-positive neurons (neurons containing hyperphosphorylated tau-protein) was determined by counting the number of AT8-positive neurons and the total number of neurons in specific brain regions.
For that reason, pictures of the AT8 stained sections were taken with Leica FireCam. From each mouse brain pictures were taken of the frontocentral cortex using the 20-fold objective and of the hippocampal CA1 region using the 40-fold objective.

Using the software Corel PHOTO-PAINT 12, each counted neuron was marked and the single marks were analyzed by Image J, Imaging Processing and Analysis Software.
The neuronal cell count in the frontocentral cortex followed particular criteria; the region determined for counting should contain at least 100 neurons and the region counted should be the one containing the most AT8-positive cells. Here, the numbers of all neurons as well as that of the AT8 positive ones were counted separately. The percentage of AT8 positive neurons was calculated as follows: $\frac{(\text{AT8 positive neurons})\text{x}100}{\text{all neurons}}$.
At 40-fold objective level all neurons in the hippocampal CA1 region seen in the respective image were counted as well as the number of AT8 positive neurons. Quantification of the AT8 positive neurons was carried out similar to that of frontocentral neurons.

2.5 Dissemination of tau pathology in the mouse brains (Braak-like staging)

To assess the expansion of tau pathology in the entire mouse brain and not only in the two specific regions that were counted, I assessed for every mouse the stage of NFT-pathology. This staging of the mice is based upon the Braak-like staging for mice according to David E. Hurtado et al. (Hurtado et al. 2010).

Stage I

The first stage is characterized by a small number of AT8-positive neurons, limited to isocortical and entorhinal regions. The isocortical expansion is limited to layers 2 and 3.

Stage II

In stage II tau-positive neurons in the cortical amygdala region and the piriform area become visible. A rare involvement of the pyramidal layer of hippocampal CA1 region or hypothalamic affection may occur.

Stage III

Beginning affection of the isocortical layer 5 can be observed in stage III. Moreover, progression of the tau pathology in the hippocampal formation becomes visible. Affected regions are the pyramidal layers of CA1 and CA3 as well as the dentate gyrus.

Stage IV

A typical finding in stage IV is the beginning affection of the striatum. Moreover, the tau pathology in the hippocampal formation appears more prominent, as indicated by newly occurring AT8-positive neurons in the strata radiatum, lucidum and oriens. A more abundant tau-pathology can be remarked in the hypothalamus, as well as AT8-positive neurons in the thalamus and midbrain.

Stage V

A beginning AT8-positive staining in neurons of the isocortical layers 4 and 6 appears in stage V.

Stage VI

In stage VI, AT8-positive neurons can be found throughout all layers of the isocortex. The hippocampal formation shows a severe positive staining; also the dentate gyrus exhibits massive accumulation of neurons containing hyperphosphorylated tau-protein. In this final stage, the abnormal tau-protein is not only found in the neuron's perikarya, but also in their processes. Furthermore, widespread neuronal loss, causing volume loss, especially in the isocortex and the hippocampal formation gets evident. This neuronal loss is accompanied by reactive astro- and microgliosis.

2.6 Dissemination of Aβ-pathology in the mouse brains (Aβ-phases)

The appearance of Aβ in the brains was detected by immunohistochemical staining with anti Aβ40 and anti Aβ42 antibodies. To determine the spread of Aβ-plaques in the brains, the sections were classified along the criteria for Aβ-phases in humans (Thal et al. 2002) as adapted for APP23 mice (Capetillo-Zarate et al. 2006; Thal et al. 2006). This staging distinguishes between different phases.

Phase 1

In phase 1 the deposition of Aβ-plaques is restricted to the neocortex.

Phase 2

Allocortical brain regions become involved in phase 2.

Phase 3

In phase 3, expansion of amyloid-β plaque depositions to nuclei of the diencephalon, the striatum and cholinergic nuclei of the basal forebrain occurs.

Phase 4

Aβ-deposits in nuclei of the midbrain and medulla oblongata appear in phase 4.

Phase 5

At last, the final phase 5 is characterized by affection of the pons and the cerebellum with amyloid-β pathology.

2.7 Protein extraction from mouse forebrain

Mouse forebrains were homogenized with homogenization buffer (TBS-Complete + PhosphoStop) to the final dilution 1:10 and sonicated. The brain homogenate samples were stored at -80°C. Further separation of the brain homogenates in different fractions was performed as described in earlier publications (Rijal Upadhaya et al. 2012) and shown in figure 1.

In short, the brain homogenates were centrifuged for 35 minutes at 4°C at 14000g. The supernatant was ultracentrifuged for 35 minutes at 4°C at 175000g. The resulting supernatant was kept as soluble fraction whereas the remaining pellet was considered to request the dispersible fraction.

The pellet which remained from the first centrifugation step was then resuspended in SDS and the resulting solution was again centrifuged for 35 minutes at 4°C at 14000g. The supernatant was kept as SDS-soluble or membrane-associated fraction. The pellet was further dissolved with 70% formic acid and kept as formic acid-soluble or plaque-associated fraction.

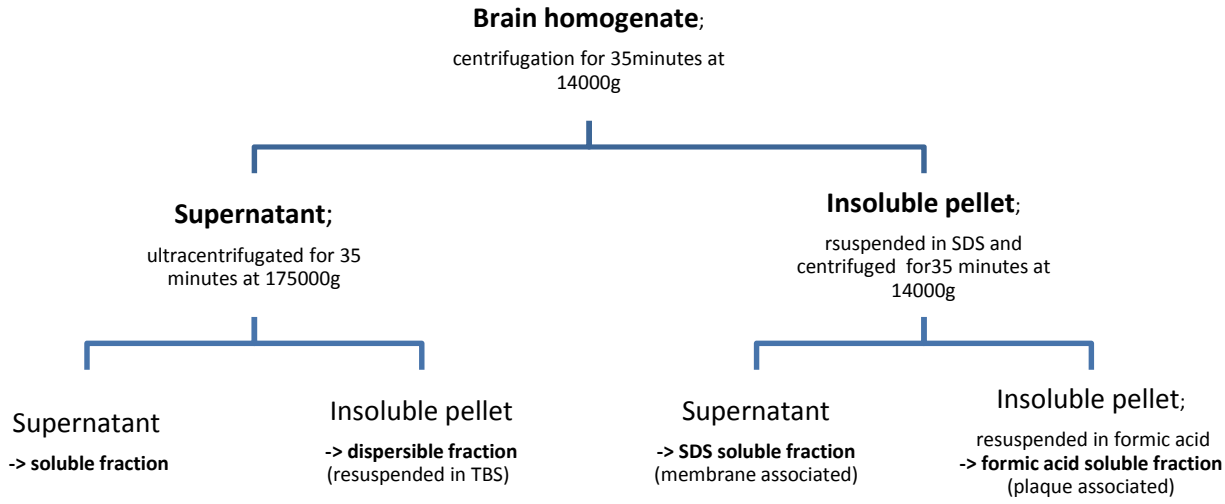

Figure 1: Separation of brain homogenates

2.8 Determination of total protein concentration

For determination of total protein concentration in the samples Pierce® BCA Protein Assay Kit was used. Each sample was 1:4 diluted with PBS buffer. From each sample, 20 µl were transferred on a 96-well plate twice. Then 8 different BSA-solutions (0µg/µl, 0.125µg/µl, 0.25µg/µl, 0.5µg/µl, 0.75µg/µl, 1µg/µl, 1.5µg/µl, 2µg/µl), twice 20µl were transferred onto the plate. These solutions serve as protein standards, which allow calculating a standard curve. To each sample 200µl of a mixture of Reagent A and Reagent B in ratio 50:1 were added. Following the plate incubated at 37°C for 30 minutes. The photometric measure of absorption at 562 nm wavelength was performed using the PowerWave 200TM microplate scanning spectrophotometer (Bio-Tek). The analysis was done with the software KC4 V3.1 (Bio-Tek Instruments, Inc., Winooski, VT, USA).

2.9 Immunoprecipitation

With immunprecipitation particular forms of the Aβ protein were purified. Therefore, two different antibodies were used; the B10AP antibody fragments, which bind to protofibrillary and fibrillary Aβ, and the A11 antibodies detecting Aβ in an oligomeric form of high molecular weight.
100µl of each, soluble and dispersible brain homogenates were incubated with 2µl of B10AP or 1µl of A11 for 5 hours at 4°C with gentle agitation. Then, 50µl of Protein G MicroBeads (Miltenyi Biotec, Bergisch-Gladbach, Germany) were added to each sample. This mixture incubated at 4°C with gentle agitation over-night. The next day, the µColumns were activated with 200µl 1% PBS-T. Afterwards, the samples were passed through the µColums, which retained the Microbead-bound antibodies (linked with its specific antigen). The microbeads were then washed with 100 µl PBS followed to elute unbound proteins and to resolve unspecific bindings of the antibodies. 20µl of 95°C hot SDS-gel loading buffer were incubated for 5 minutes with each of the µColumns prior to eluting the microbead-bound proteins with 200µl of 95°C preheated SDS-gel loading buffer.

2.10 SDS-PAGE and Western blot

For SDS-PAGE and subsequent Western blot analysis, the different protein fractions as well as the immunoprecipitated samples from APP23xTAU58/2, APP51/16xTAU58/2, APP48xTAU58/2 and TAU58/2 mice were used. From each group a number of six mice were examined. All mice were 6 months old (see table 9).

The SDS-PAGE was performed using a NuPAGE 4-12% Bis-tris gel system (Invitrogen) with 1% MES-SDS running buffer (Invitrogen). The immunoprecipitated samples were directly loaded onto the gel (15µl each), whereas the other samples required a pretreatment. For this purpose, we took 10µl of the sample and mixed it with 3.75µl LDS sample buffer and 1.5µl Reducing Agent. The mixture was heated at 70°C for 10 minutes and following loaded onto the gel by adding 200µl of antioxidant to every chamber. The gel ran at 150 V for 55 minutes.

The resolved proteins were transferred to a nitrocellulose membrane. For the transfer buffer we mixed 140 ml 10% transfer buffer, 200 ml methanol and 1160 ml aqua dest. The blotting was performed with 250V, 0.4 A for 2 hours.

After blotting the membranes were boiled with PBS for 5 minutes in the microwave and blocked in 5% non-fat dry milk (Roth, Karlsruhe, Germany), which was diluted in antibody-dilution buffer for 1 h at room temperature. After three washing steps in PBS-T (each 10 minutes), the membranes were incubated with the primary antibody at 4°C with gentle agitation over-night.

For detecting amyloid β we used 6E10 antibody (1:1000), which is a monoclonal mouse antibody raised against Aβ 1-17. After the incubation with the primary antibody, the membranes were washed again for three times in PBS-T before incubating with the secondary antibody MS-HRP for 2h at room temperature with gentle agitation. A last washing step followed. Finally, the blots were developed using an enhanced chemiluminescence (ECL) detection system (Supersignal Pico Western system, Thermo Scientific-Pierce, Waltham, MA, USA) and illuminated in ECL hyperfilm (GE Healthcare, Buckinghamshire, UK).

Quantification of Western blots

For the quantification of the Western blots Image J software was used. An area around the bands, which should be quantified was selected with the "Rectangular Select" tool. This box was then dragged, so that the next bands were also selected in the boxes. By doing so, histograms could be generated, which show the intensity of the different bands. With the "Magic Wand" tool the intensity of the bands is presented as a numerical value. This value correlates with the protein content represented by a respective band.

2.11 Phospho tau and total tau ELISA

The protein concentration of the samples used for ELISA was determined with the Pierce® BCA Protein Assay as described in 2.8. For determination of the levels of tau and phosphorylated tau in the mouse brains a total of 28 mice brains were examined. ELISA measurement of total and phospho tau was carried out for the mice listed in table 10.
For ELISA measurements a MSD® MULTI-SPOT Phospho (Thr231)/ Total Tau Assay was used. First 150µl of Blocker A solution was added to each of the 96 wells and incubated for one hour followed by four washing steps with 150µl of 1X Tris Wash Buffer. Next the calibrator samples and the mouse samples were added to the wells and incubated for one hour. After that, the plate was washed four times with 1X Tris Washing Buffer. Now, the detection antibody solution was added to each well for one hour. After a last washing step, the diluted Read Buffer T was added and the analysis with the MSD instrument followed. All samples were measured in duplicates. The mean values of the calculated concentrations were used for further analysis of the ELISA-data.

2.12 Statistical analysis

For calculating statistical tests IBM SPSS Statistics 21 and 24 software was used. Kruskal Wallis test followed by Dunn-Bonferroni post-hoc test was calculated for comparison of the mean values of the percentage of AT8-positive neurons among the three different

genotypes (APP23xTAU58, APP48xTAU58, APP51/16xTAU58) and the control group, the TAU58/2 mice. This test was used, because not all of the measurements showed normal distribution.

To show differences between each of the three genotypes and the control group (TAU58/2) in the Braak-like staging, Mann-Whitney-U-test corrected for multiple testing was used with a level of significance 0,05.

To compare the levels of Aβ among the different genotypes (APP23xTAU58, APP48xTAU58, APP51/16xTAU58, TAU58/2) determined by Western blotting Kruskal Wallis test followed by Dunn-Bonferroni post-hoc test was performed.

The results of the ELISA analyses were evaluated the same way as the Western blot results using Kruskal Wallis test followed by Dunn-Bonferroni post-hoc test.

3. Results

Differences were found, not only in the extent of the tau pathology but also in the biochemical profiles of Aβ aggregates in different fractions of brain homogenates between the different mouse lines. First, the neuropathological differences between the different double and single transgenic mouse lines will be described, followed by the differences regarding the biochemical pattern of Aβ aggregates.

3.1 Neuropathological findings in TAU58/2, APP23xTAU58/2, APP51/16xTAU58/2 and APP48xTAU58/2 mice

Neuropathological findings in TAU58/2 mice

In line with earlier findings, neurofibrillary tangles can be detected in TAU58/2 mice at the age of 6 months in the Gallyas silver staining (see figure 2). The neurofibrillary tangles mainly occur in the frontocentral cortex as well as in brainstem nuclei.

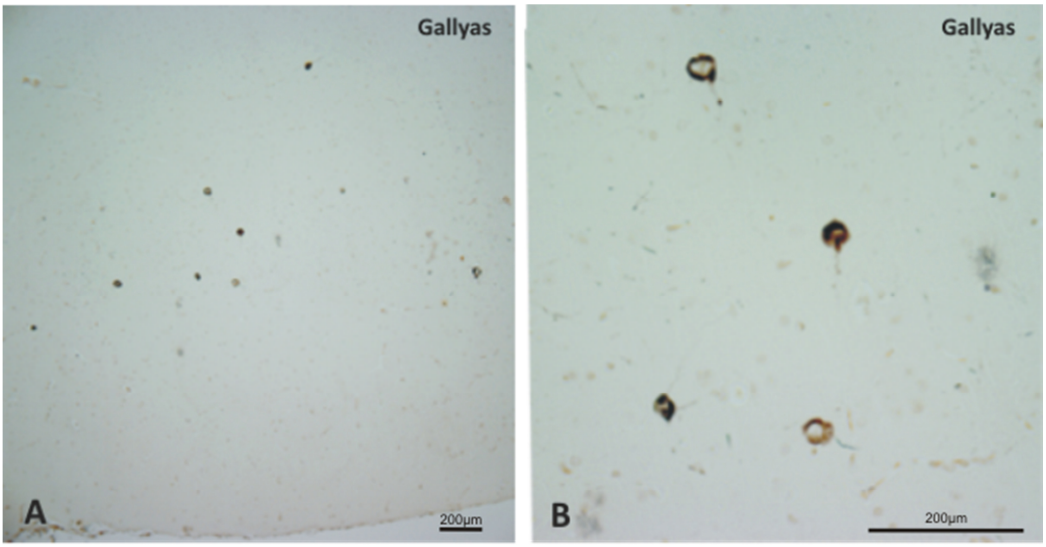

Figure 2: Gallyas silver staining of a 6 months old TAU58/2 mouse. A) Frontocentral cortex in 20-fold magnification. Multiple neurofibrillary tangles can be seen. B) Frontocentral cortex in 40-fold magnification. Some of the neurofibrillary tangles seen in A) are shown in detail.

Likewise, in immunohistochemical stainings with the AT8 antibody (detecting hyperphosphorylated tau protein) pretangles, neuropil threads and tangles can be seen in the same brain regions where the tangles are seen in the Gallyas silver staining, presenting with a prominent staining especially in the frontocentral cortex as well as in the hippocampal CA1 region.

These tau lesions mainly consist of four-repeat tau, as indicated by the staining of neurons exhibiting pretangles and tangles with the RD4 antibody, detecting specifically four-repeat tau. In contrast, staining with the RD3 antibody (detecting three-repeat tau) reveals no positive staining (see figure 3).

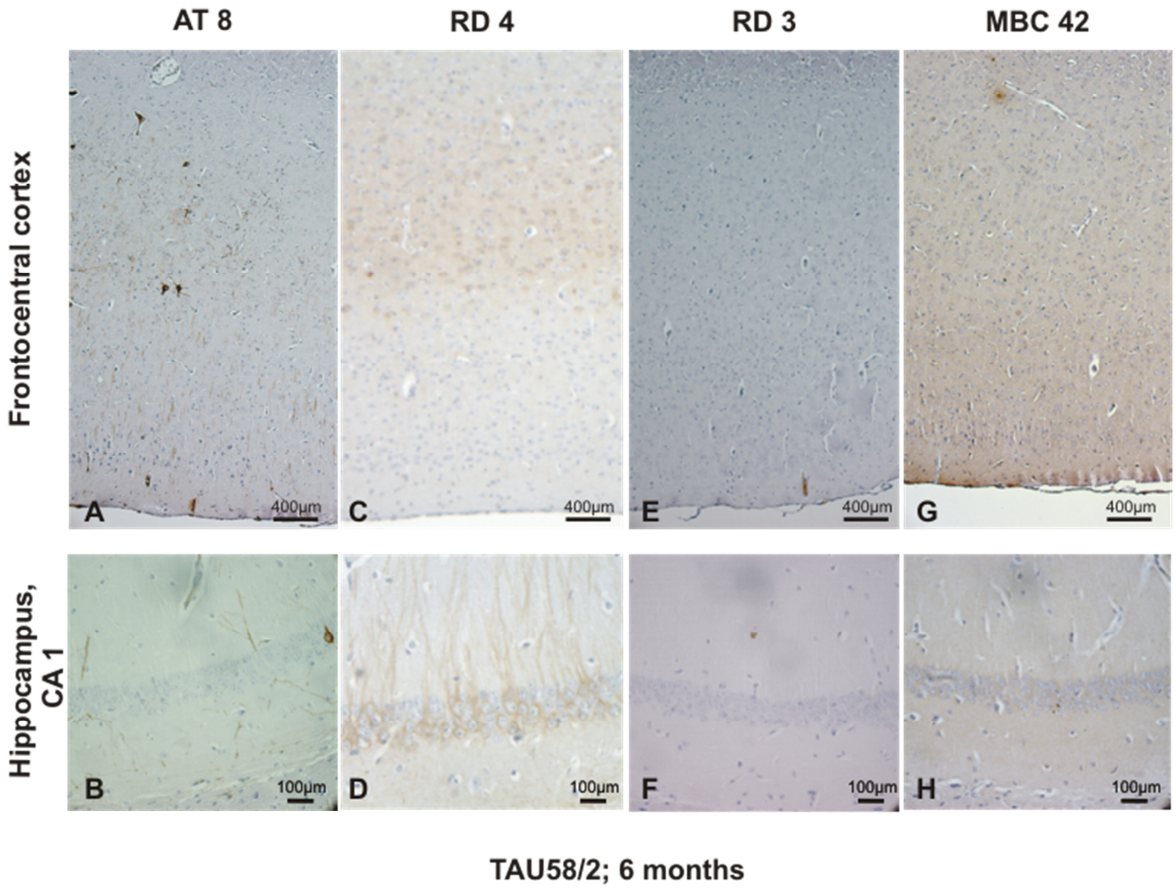

Figure 3: Overview of the different immunohistochemical stainings in 6 months old TAU58/2 mice.
A) Frontocentral cortex, staining with the AT8 antibody. Several neurons show a positive staining. Also in B) the hippocampal CA1 region, positive stained neurons can be found. C) Staining with the RD4 antibody reveals neurons containing 4-repeat tau in the frontocental cortex as well as in the D) hippocampal CA1 region. Staining with the RD3 antibody does not show aggregates of 3-repeat tau, neither in the E) frontocentral cortex, nor in the F) hippocampal CA1 region. Immunohistochemical staining with the anti Aβ42 antibody does not show Aβ plaques in the G) frontocentral cortex or the H) hippocampal CA1 region.

By counting AT8 positive neurons, TAU58/2 mice present with lower percentage amounts of AT8 positive neurons in the frontocentral cortex compared to APP23xTAU58/2 mice (Kruskal Wallis test with Dunn-Bonferroni post-hoc test, z=3,533, p=0,002; APP23xTAU58/2 n=10, TAU58/2 n=18). In comparison to APP51/16xTAU58/2 and APP48xTAU58/2 mice no significant differences can be seen (see figure 4 and figure 5).

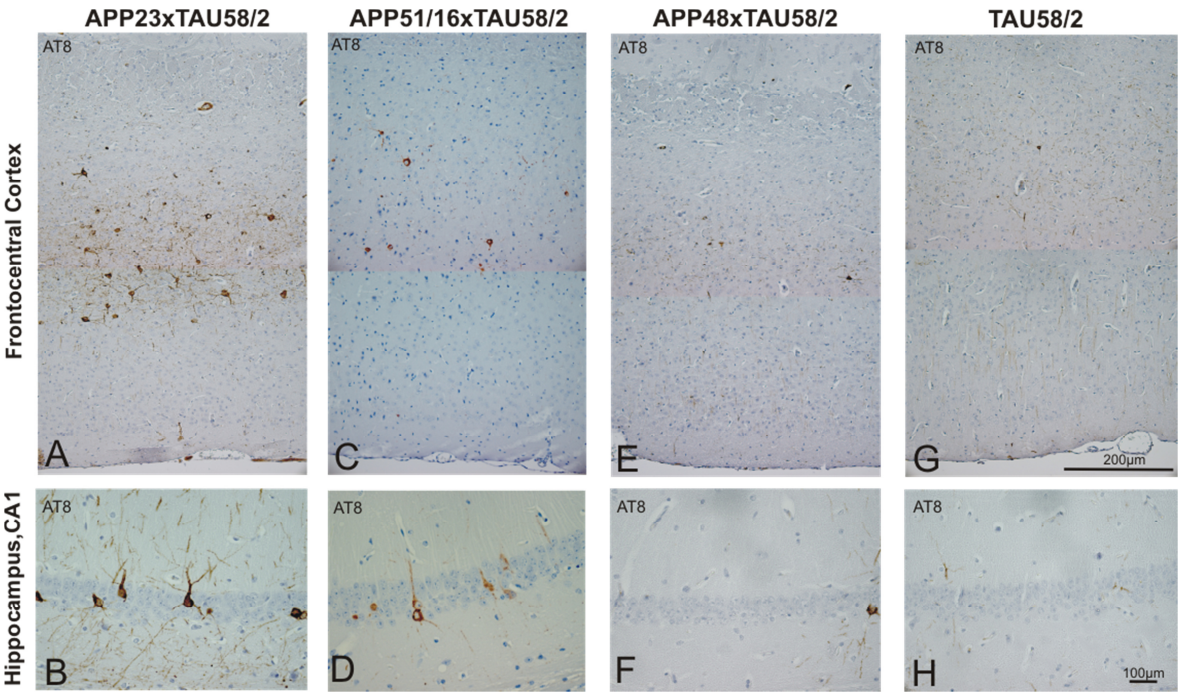

Figure 4: Immunohistochemical staining with the AT8 antibody. A) APP23xTAU58/2, frontocentral cortex. The same mouse shows serve hippocampal affection, B) Hippocampus CA1. C) The APP51/16xTAU58/2 mice show lower numbers of AT8 positive neurons in the frontocentral cortex than the APP23xTAU58/2 mice, whereas these animals also show serve hippocampal tau pathology. D) APP51/16xTAU58/2 Hippocampus CA1. E) APP48xTAU58/2 mice only show rare AT8 positive neurons in the frontocentral cortex as well as in the hippocampal CA1 region F). G) TAU58/2 mice show tau pathology to a minor degree as well in the frontocentral cortex, as in the hippocampal CA1 region, H).

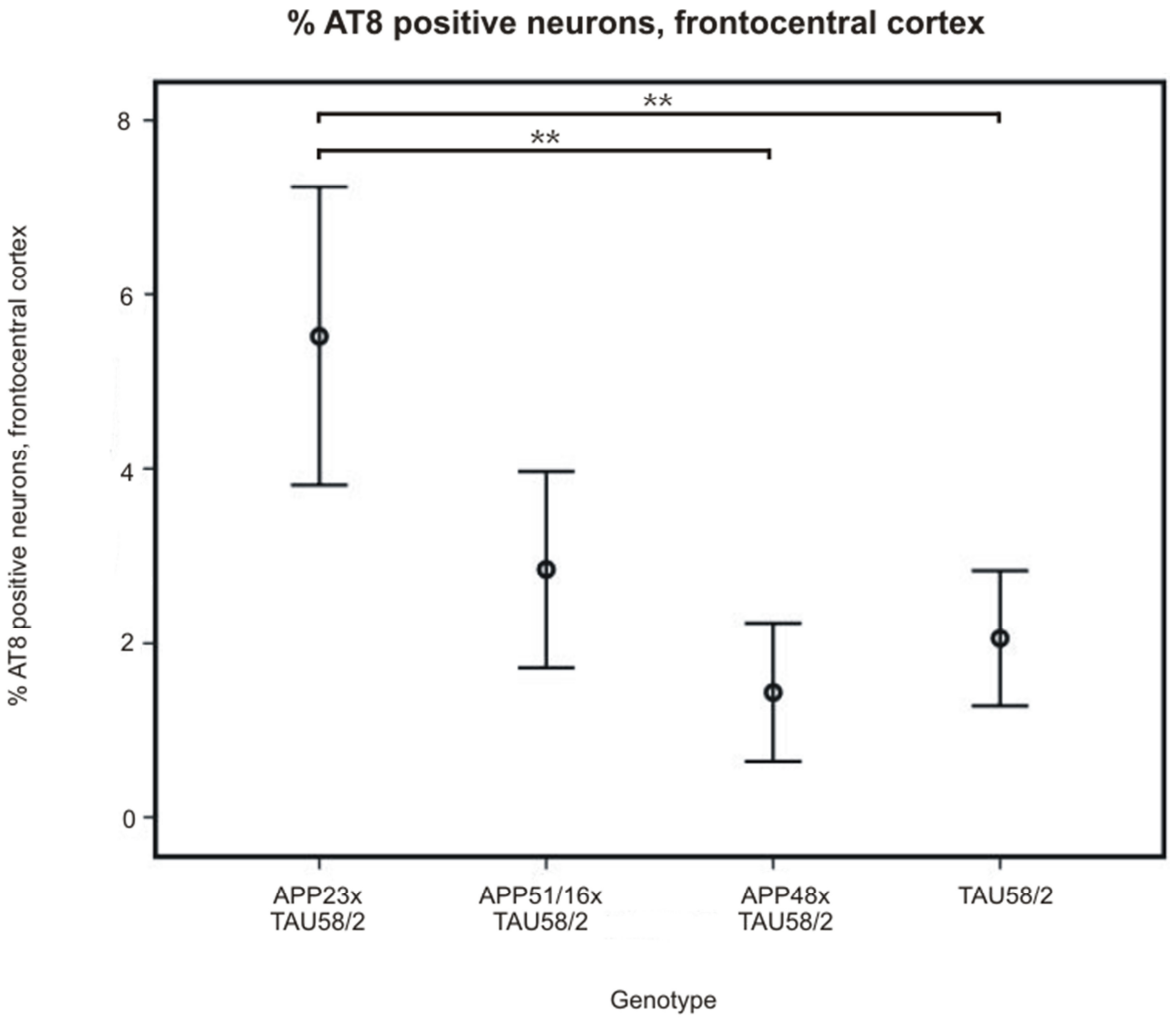

Figure 5: Percentage of neurons containing hyperphosphorylated tau protein in the frontocentral cortex, detected with AT8 staining

Neuronal cell count was performed in APP23xTAU58/2 n=10, APP51/16xTAU58/2 n=8, APP48xTAU58/2 n=9 and TAU58/2 n=18 mice.

APP23xTAU58/2 mice show a significant higher percentage of AT8 positive neurons in the frontocentral cortex than APP48xTAU58/2 and TAU58/2 mice.

(Kruskal Wallis test with Dunn-Bonferroni post-hoc test: ** $p \leq 0.01$; n = 10 for each group, except APP51/16xTAU58/2 n=7 and TAU58/2 n=18 mean and standard errors are presented).

In the hippocampal CA1 region, TAU58/2 mice show significantly lower numbers of AT8 positive neurons compared to APP23xTAU58/2 (Kruskal Wallis test with Dunn-Bonferroni post-hoc test, z=3,707, p=0,01; APP23xTAU58/2 n=10, TAU58/2 n=18) and APP51/16xTAU58/2 mice (Kruskal Wallis test with Dunn-Bonferroni post-hoc test, z=2,837, p=0,027; APP51/16xTAU58/2 n=8, TAU58/2 n=18) (see figure 4 and figure 6).

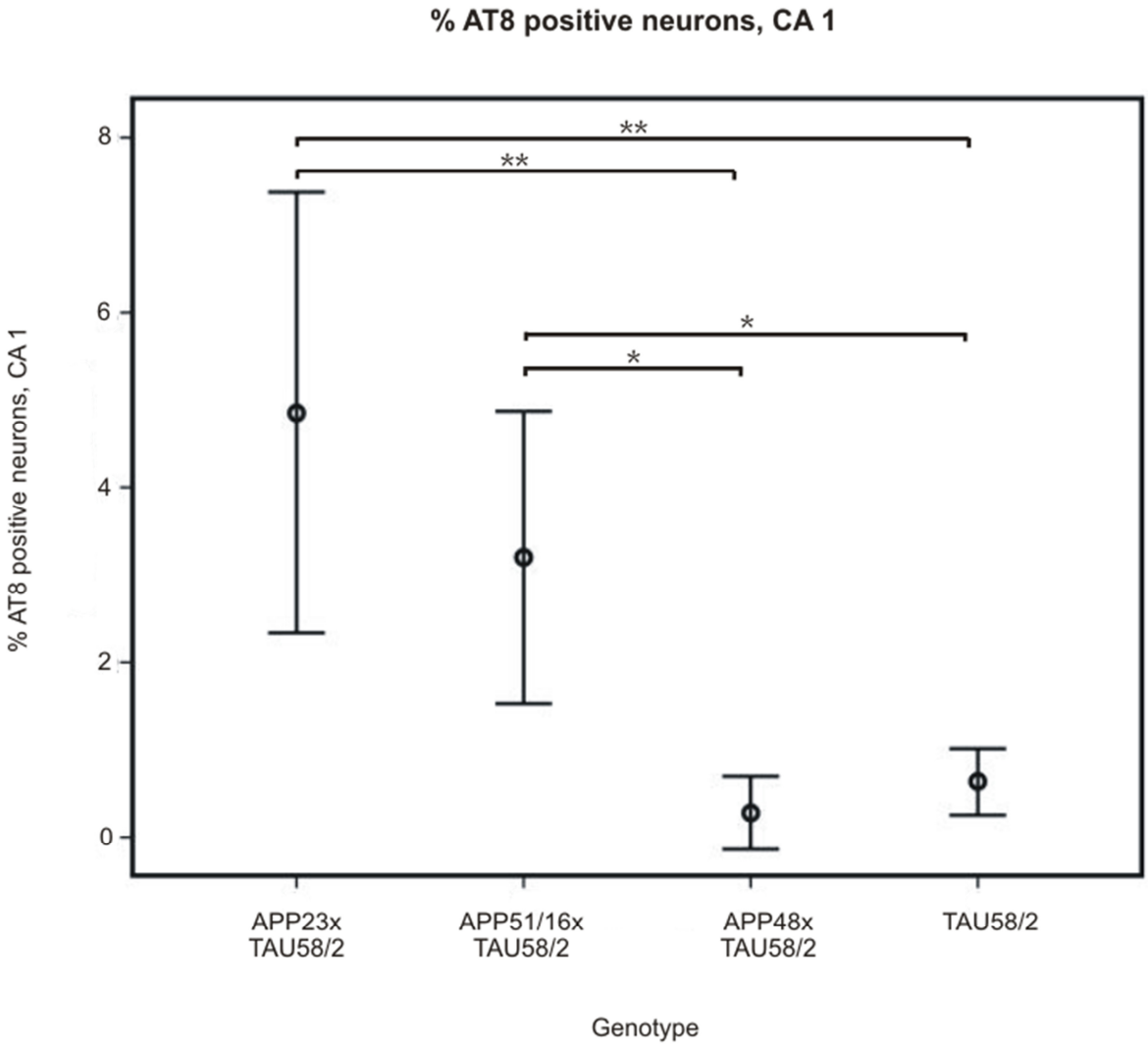

Figure 6: Percentage of neurons containing hyperphosphorylated tau protein in the CA1 section of the hippocampus, detected with AT8 staining

Neuronal cell count was performed in APP23xTAU58/2 n=10, APP51/16xTAU58/2 n=8, APP48xTAU58/2 n=9 and TAU58/2 n=18 mice.

APP23xTAU58/2 mice show a significant higher percentage of AT8 positive neuron in the hippocampal CA1 region than APP48xTAU58/2 and TAU58/2 mice. APP51/16xTAU58/2 mice show a significant higher number of AT8 positive neuron in the hippocampal CA1 region than APP48xTAU58/2 and TAU58/2 mice.

(Kruskal Wallis test with Dunn-Bonferroni post-hoc test: * p<0,05; ** p<0,01; n=10 for each group, except APP51/16xTAU58/2 n=7 and TAU58/2 n=18. Mean and standard errors are presented).

In the Braak-like staging TAU58/2 mice show lower stages than APP23xTAU58/2 mice (Mann-Whitney test, exact 2-tailed significance p=0,00; APP23xTAU58/2 n=10, TAU58/2 n=18). In comparison to APP51/16xTAU58/2 and APP48xTAU58/2 mice again no significant difference is detected (see figure 7).

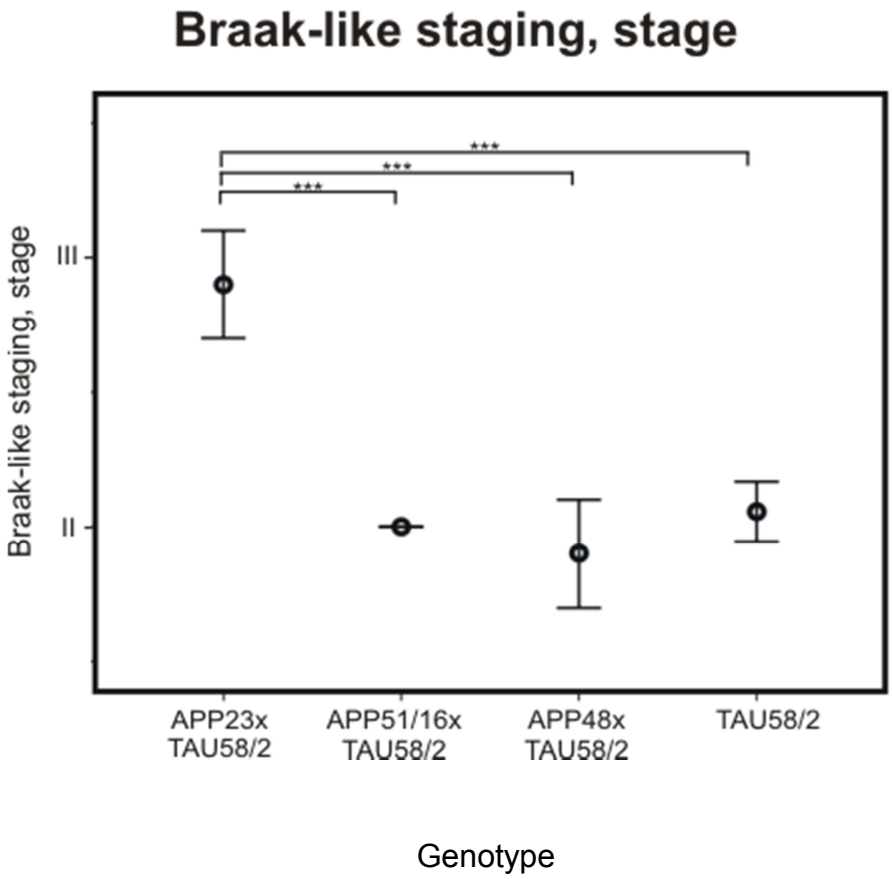

Figure 7: Braak-like staging based upon the AT8 staining
The staging was performed in APP23xTAU58/2 n=10, APP51/16xTAU58/2 n=8, APP48xTAU58/2 n=9 and TAU58/2 n=18 mice.
APP23xTAU58/2 mice show significant higher stages than APP51/16xTAU58/2, APP48xTAU58/2 and TAU58/2 mice.
(Tested with Mann-Whitney Test: *** exact 2-tailed significance < 0,001; n=10 for each group, except APP51/16xTAU58/2 n=7 and TAU58/2 n=18. Mean and standard errors are presented).

In immunohistochemical staining with anti Aβ40 and anti Aβ42 antibodies, no Aβ plaques are found in TAU58/2 mice (see figure 3).

Neuropathological findings in APP23xTAU58/2 mice

APP23xTAU58/2 mice also present with neurofibrillary tangles consisting of four-repeat tau and four-repeat tau expressing neurons detected in immunohistochemical staining with the RD4 antibody (see figure 4). Staining with the RD3 antibody reveals no aggregates of three-repeat tau, comparable to TAU58/2 mice (see figure 8).

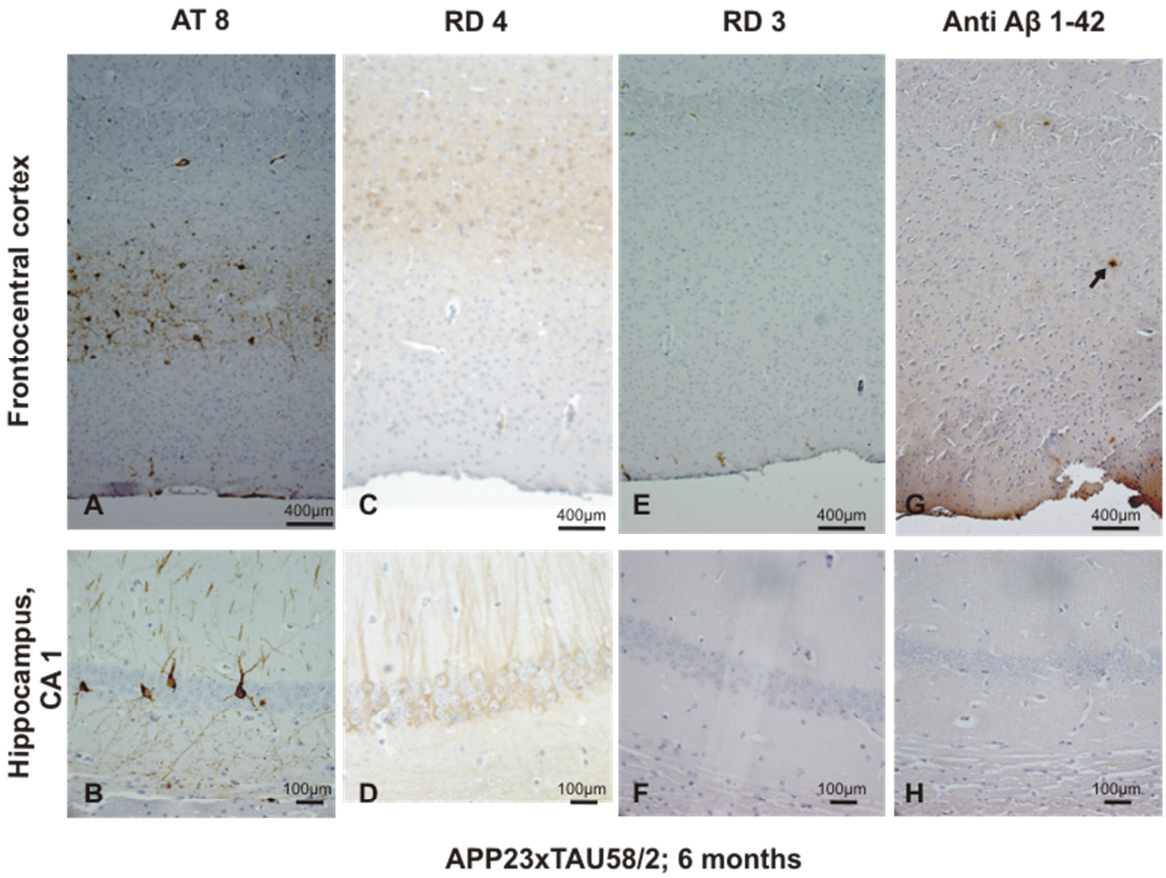

Figure 8: Overview of the different immunohistochemical stainings in 6 months old APP23xTAU58/2 mice.
A) More distinct tau pathology in the AT8 staining can be seen in the frontocentral cortex as well as in the B) hippocampal CA1 region compared to the other mouse models. As in TAU58/2 mice, increased levels of 4-repeat tau can be detected with the RD4 staining in the C) frontocentral cortex and in the D) hippocampal CA1 region; but no 3-repeat tau gets visible in staining with the RD3 antibody, neither in the E) frontocentral cortex, nor in the F) hippocampal CA1 region. One animal showed a single Aβ plaque in the G) frontocentral cortex (marked with an arrow), in the H) hippocampal CA1 region no staining can be detected with anti Aβ42 antibody.

In contrast to TAU58/2 mice, APP23xTAU58/2 mice show more distinct tau pathology. In neuronal cell count of AT8 positive neurons they provide the highest number of positively stained neurons in the frontocentral cortex although the difference is only significant in comparison with APP48xTAU58/2 mice (Kruskal Wallis test with Dunn-Bonferroni post-hoc test, z=3,76, p=0,001; APP23xTAU58/2 n=10, APP48xTAU58/2 n=9) and TAU58/2 mice (Kruskal Wallis test with Dunn-Bonferroni post-hoc test, z=3,533 p=0,002; APP23xTAU58/2 n=10, TAU58/2 n=18) (see figure 4 and figure 5).
Also in the hippocampal CA1 region, APP23xTAU58/2 mice show the highest numbers of neurons containing hyperphosphorylated tau protein, detectable with the AT8 antibody. As in the frontocentral cortex, the APP23xTAU58/2 also exhibit higher numbers of AT8

positive neurons than the APP48xTAU58/2 mice (Kruskal Wallis test with Dunn-Bonferroni post-hoc test, z=3,895, p=0,001; APP23xTAU58/2 n=10, APP48xTAU58/2 n=9) and TAU58/2 mice (Kruskal Wallis test with Dunn-Bonferroni post-hoc test, z= 3,707, p=0,001; APP23xTAU58/2 n=10, TAU58/2 n=18) (see figure 4 and figure 6). Furthermore, a stronger staining of the neuropil can be noticed in the APP23xTAU58/2 mice compared to the other animal models (see figure 8 and figure 4).

The finding that tau pathology in APP23xTAU58/2 mice is more pronounced than in the other mouse models is confirmed by the Braak-like staging based upon the AT8 staining. Here, the APP23xTAU58/2 mice show significantly higher stages than APP51/16xTAU58/2 (Mann-Whitney test, exact 2-tailed significance p=0,000; APP23xTAU58/2 n=10, APP51/16xTAU58/2 n=8), APP48xTAU58/2 (Mann-Whitney test, exact 2-tailed significance p=0,00; APP23xTAU58/2 n=10, APP48xTAU58/2 n=9) and TAU58/2 mice (Mann-Whitney test, exact 2-tailed significance p=0,00; APP23xTAU58/2 n=10, TAU58/2 n=18) (see figure 7).

In the immunohistochemical staining with anti Aβ40 and anti Aβ42 antibodies, only one of the examined animals exhibits single plaques in the neocortex, representing phase 1 in the Aβ phases (see figure 8). The other animals do not exhibit Aβ plaques.

Neuropathological findings in APP51/16xTAU58/2 mice

Neurofibrillary tangles detectable with AT8 and RD4 immunohistochemical staining techniques can also be seen in APP51/16xTAU58/2 mice (see figure 9). Four-repeat tau was expressed in the neurons of these mice. Three-repeat tau was not detectable in the aggregates as well as in neurons.

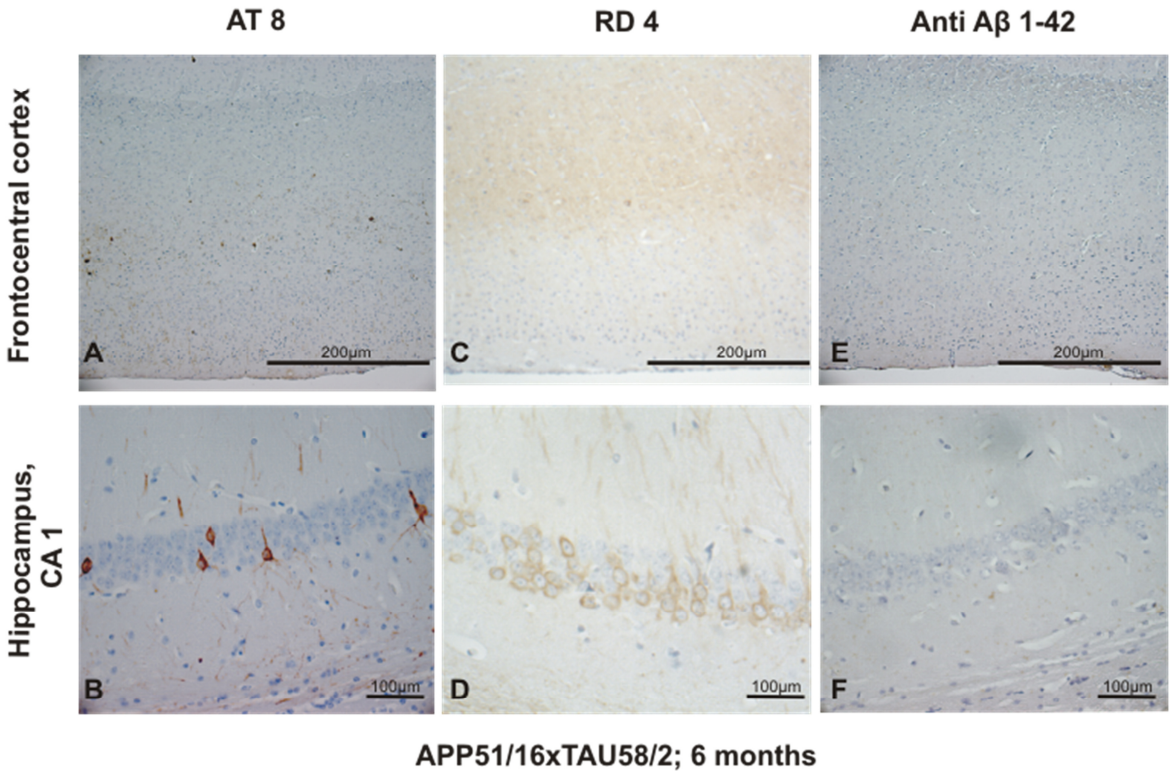

Figure 9: Overview of the different immunohistochemical stainings in 6 months old APP51/16xTAU58/2 mice.

A) AT8 staining shows clearly stained neurons in the frontocentral cortex, as well as in the B) hippocampal CA1 region. Again RD4 staining reveals the occurrence of 4-repeat tau in the C) frontocentral cortex and in the D) hippocampal CA1 region. In APP51/16xTAU58/2 mice no positive staining with RD3 can be seen like in TAU58/2 and APP23xTAU58/2 mice (not shown). Also staining with MBC 42 antibody does neither show aggregates of Aβ in the E) frontocentral cortex, nor in the F) hippocampal CA1 region.

The percentage of AT8 positive neurons in the frontocentral cortex of APP51/16xTAU58/2 mice is lower as in APP23xTAU58/2 mice. But the difference is not significant; neither in the frontocentral cortex, nor in the hippocampal CA1 region. In the hippocampal CA1 region APP51/16xTAU58/2 mice show a higher number of neurons containing hyperphosphorylated tau protein, detected with the AT8 antibody than APP48xTAU58/2 (Kruskal Wallis test with Dunn-Bonferroni post-hoc test, z=3,131, p=0,01; APP51/16xTAU58/2 n=8, APP48xTAU58/2 n=9) and TAU58/2 mice (Kruskal Wallis test with Dunn-Bonferroni post-hoc test, z=2,837, p=0,027; APP51/16xTAU58/2 n=8, TAU58/2 n=18) (see figure 4 and figure 6).

In the Braak-like staging APP51/16xTAU58/2 mice do not differ from APP48xTAU58/2 and TAU58/2 mice. Compared to APP23xTAU58/2 mice, APP51/16xTAU58/2 mice show lower stages (Mann-Whitney test, exact 2-tailed significance p=0,00; APP23xTAU58/2 n=10, TAU58/2 n=18) in the Braak-like staging (see figure 7) .

In immunohistochemical staining with anti Aβ40 and anti Aβ42 antibodies, no Aβ plaques are found (see figure 9).

Neuropathological findings in APP48xTAU58/2 mice

In line with TAU58/2, APP23xTAU58/2 and APP51/16xTAU58/2 mice, in APP48xTAU58/2 mice four-repeat tau was expressed in neurons, whereas three-repeat tau was not detectable in the aggregates as well as in neurons (see figure 10).

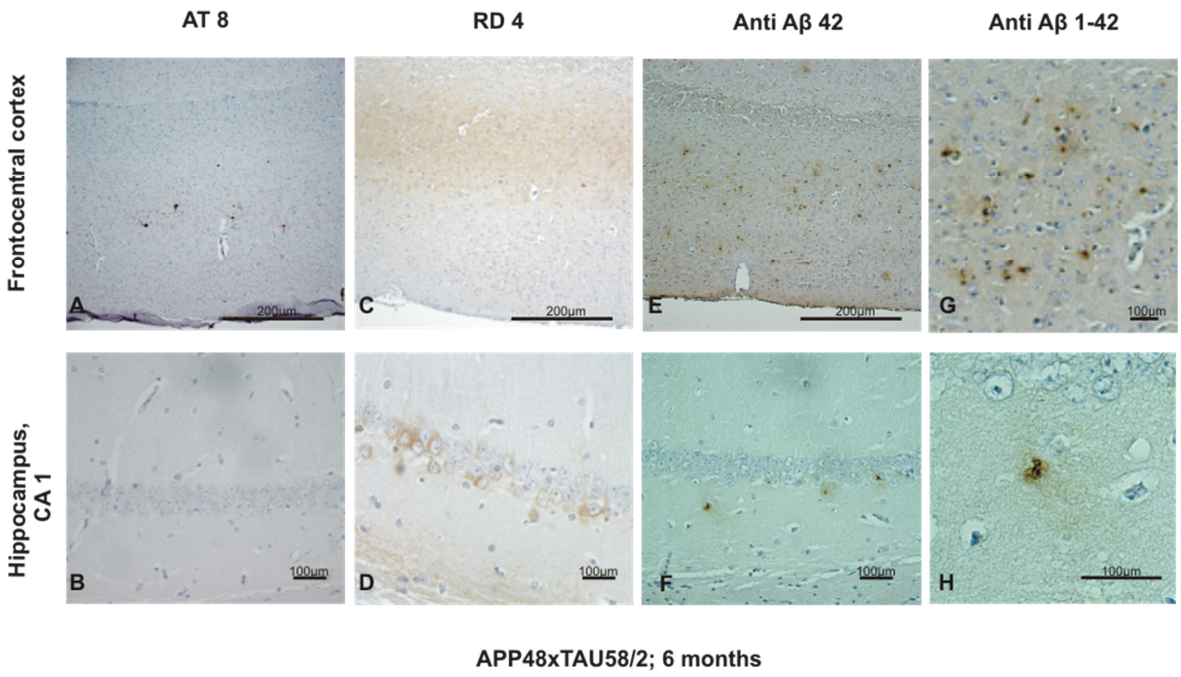

Figure 10: Overview of the different immunohistochemical stainings in 6 months old APP48xTAU58/2 mice.
A) AT8 staining shows clearly stained neurons in the frontocentral cortex; in the B) hippocampal CA1 region no positive staining can be seen. Again the RD4 staining reveals the occurrence of 4-repeat tau in the C) frontocentral cortex and in the D) hippocampal CA1 region. In APP48xTAU58/2 mice no positive staining with the RD3 antibody is seen like in TAU58/2 and APP23xTAU58/2 mice (not shown). Staining with anti Aβ42 antibody shows accumulations of Aβ in the E) frontocentral cortex and in the F) hippocampal CA1 region. These aggregates do only occur intracellular and can hence not be defined as Aβ plaque. G) Shows a detail from E) showing the intracellular Aβ deposits. H) Shows intracellular Aβ as a detail from F).

A similar distinction of AT8 positive neurons is seen in APP48xTAU58/2 mice as in TAU58/2 mice. The number of AT8 positive cells in the frontocentral cortex is lower than in APP23xTAU58/2 mice (Kruskal Wallis test with Dunn-Bonferroni post-hoc test, z=3,76, p=0,001; APP48xTAU58/2 n=9, APP23xTAU58/2 n=10) (see figure 4 and figure 5).

In the hippocampal CA1 region APP48xTAU58/2 mice also exhibit lower numbers of AT8 positive neurons than APP23xTAU58/2 (Kruskal Wallis test with Dunn-Bonferroni post-hoc test, z=3,895, p=0,001; APP48xTAU58/2 n=9, APP23xTAU58/2 n=10) and APP51/16xTAU58/2 mice (Kruskal Wallis test with Dunn-Bonferroni post-hoc test, z=3,131, p=0,01; APP48xTAU58/2 n=9, APP51/16xTAU58/2 n=8) (see figure 4 and figure 6).

In the Braak-like staging only a difference to APP23xTAU58/2 mice can be detected. APP48xTAU58/2 mice have lower stages than APP23xTAU58/2 mice (Mann-Whitney test, exact 2-tailed significance p=0,00; APP23xTAU58/2 n=10, TAU58/2 n=18) (see figure 7) .

Immunohistochemical staining with anti Aβ40 and anti Aβ42 antibodies reveals no Aβ plaques. Instead intracellular accumulations of Aβ can be seen (see figure 10).

Figure 11 again summarizes the histopathological findings in the different mouse models.

Mouse Model	n	Aβ expression	Aβ phase	RD4	RD3	%AT8+ neurons FC (mean)	%AT8+ neurons CA1 (mean)	Braak-stage
TAU58/2	18	-	-	Positive stained neurons in FC and CA1	-	2,06 (SD=1,51)	0,6 (SD=0,72)	Stage I/II n=1 Stage II n=16 Stage III n=1
APP23x TAU58/2	10	Overexpression of mutated human APP (Swedish mutation)	One single animal phase 1	Positive stained neurons in FC and CA1	-	5,53 (SD=2,27)	4,86 (SD=3,34)	Stage II n=1 Stage III n=9
APP51/16x TAU58/2	8	Overexpression of human wildtype APP	-	Positive stained neurons in FC and CA1	-	2,85 (SD=1,26)	3,2 (SD=2,17)	Stage II n=8
APP48x TAU58/2	10	Synthesis of Aβ in the endoplasmic reticulum (-> only intracellular Aβ)	-	Positive stained neurons in FC and CA1	-	1,44 (SD=0,98)	0,28 (SD=0,56)	Stage I/II n=1 Stage II n=9

Figure 11: Overview over the neuropathological findings in TAU58/2 (n=18), APP23xTAU58/2 (n=10), APP51/16xTAU58/2 (n=8) and APP48xTAU58/2 (n=18) mice. FC= frontocentral cortex, SD= standard deviation.

3.2 Intraneuronal colocalization of Aβ/APP and hyperphosphorylated tau

To clarify whether neuronal tau pathology can be related to intraneuronal Aβ or APP, immunofluorescent double staining with anti Aβ (4G8, Aβ42) and anti phospho-tau-antibodies (AT8) was performed; here, intraneuronal colocalization of Aβ or APP and abnormally phosphorylated tau protein in APP23xTAU58/2 and APP51/16xTAU58/2 as is seen. In APP48xTAU58/2 mice a colocalization of hyperphosphorylated tau and Aβ is evident. This colocalization is not seen in all of the neurons containing hyperphosphorylated tau, but in some. With immunohistochemical staining using anti Aβ42 antibody we also see intraneuronal aggregations of the Aβ protein in all three Aβ-producing mouse lines. This confirms the immunofluorescence detection of Aβ (see Figure 12). When using 4G8 for the double staining APP is stained as well.

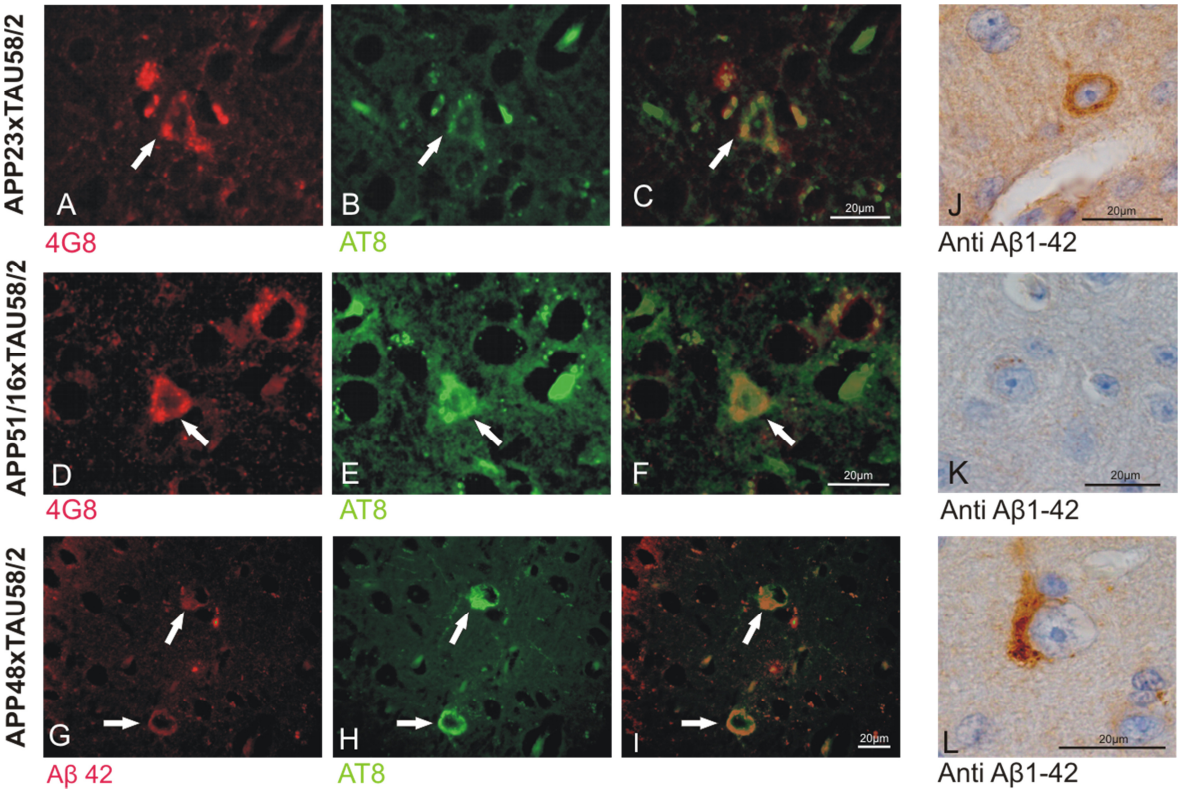

Figure 12: Immunofluorescence double staining shows colocalization of Aβ and abnormally phosphorylated tau protein in neurons. A) Aβ positive material in neocortical neurons of APP23xTAU58/2 mice (staining with 4G8, 100-fold). B) AT8 positive neocortical neurons in APP23xTAU58/2 mice. C) Overlap of A and B. The yellow areas (arrows) show the colocalization of Aβ and abnormally phosphorylated tau protein. D) 4G8 positive neocortical neurons in APP51/16xTAU58/2 mice. E) AT8 positive neocortical neurons in APP51/16xTAU58/2 mice. F) Overlap of D and E. The yellow areas show the colocalization of Aβ and abnormally phosphorylated tau protein in APP51/16xTAU58/2. G) Neocortical neurons of APP48xTAU58/2 mice showing positive signals with Aβ 42 staining, 100-fold. H) The same cells also show AT8 positive signals. I) With overlapping of G and H neuronal regions containing Aβ as well as abnormally phosphorylated tau protein become visible as yellow areas. With immunohistochemical staining using anti Aβ 42 antibody we also see intraneuronal aggregations of the Aβ protein in J) APP23xTAU58/2, K) APP51/16xTAU58/2 and L) APP48xTAU58/2 mice, which proves that the immunofluorescence staining is not unspecific.

3.3 Biochemical differences of Aβ content in the different mouse models

To determine the content of Aβ in the different brain fractions derived from brain homogenates, i.e. the soluble, dispersible, membrane associated and plaque associated fraction, respectively, Western blot analyses were performed. To detect Aβ the 6E10 antibody was used.

Aβ in the soluble fraction

In Western blot analyses with the 6E10 antibody of the soluble fraction, APP23xTAU58/2 mice show the most distinct Aβ bands. A significant difference can be detected between APP23xTAU58/2 and TAU58/2 mice (Kruskal Wallis test with Dunn-Bonferroni post-hoc test, z=3,878, p=0,001; APP23xTAU58/2 n=6, TAU58/2 n=6), and between APP23xTAU58/2 and APP48xTAU58/2 mice (Kruskal Wallis test with Dunn-Bonferroni post-hoc test, z=3,47, p=0,003; APP23xTAU58/2 n=6, APP48xTAU58/2 n=6), with APP23xTAU58/2 mice containing more Aβ (see figure 13).
In APP51/16xTAU58/2 mice, Western blot analyses with the 6E10 antibody of the soluble fraction does not show significant differences of the amount of Aβ in comparison to the other tested mouse models (see figure 13), although the Aβ bands are stronger stained compared to the Aβ bands seen in APP48xTAU58/2 and TAU58/2 mice.
APP48xTAU58/2 and TAU58/2 mice present with the lowest content of Aβ (see figure 13).

A)

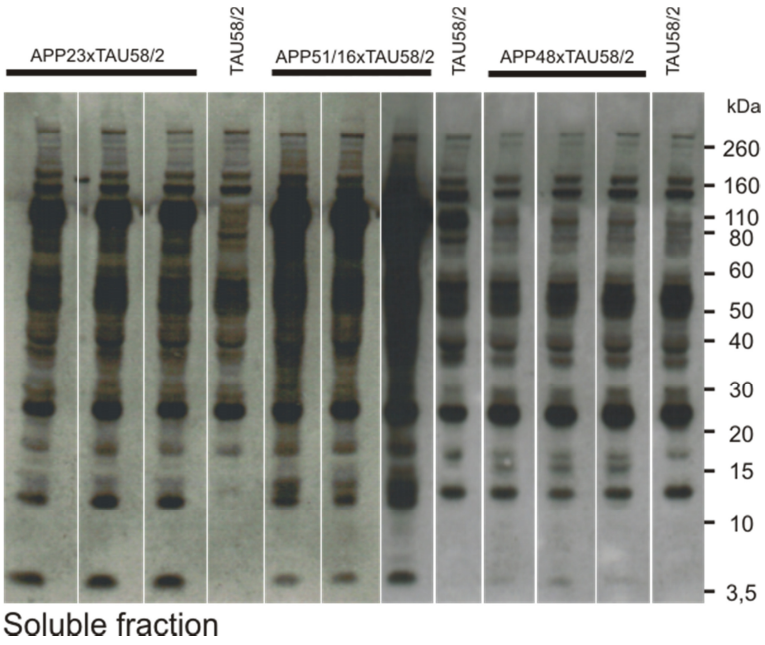

B)

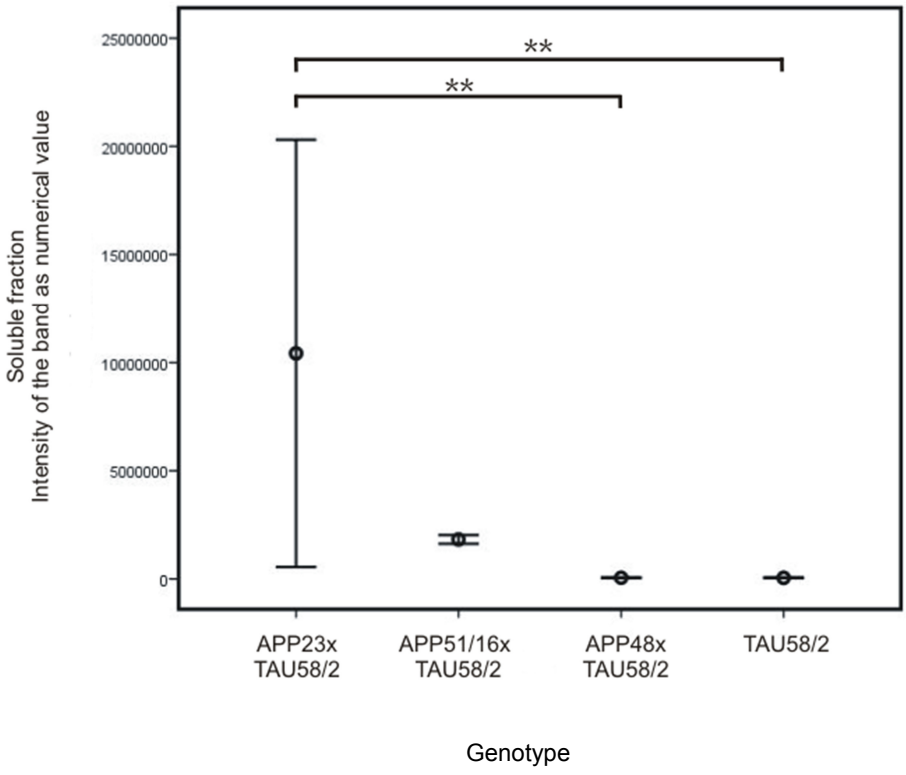

Figure 13: A) Western blot analysis of Aβ in the soluble fraction of the different mouse models. For detection of Aβ the 6E10 antibody was used. Aβ occurs as 4kDa molecular weight band. B) Kruskal Wallis test with Dunn-Bonferroni post-hoc test: ** $p < 0.01$; n = 6 for each group, mean and standard errors are presented. APP23xTAU58/2 mice show significant stronger signals than APP48xTAU58/2 and TAU58/2 mice.

Aβ in the soluble fraction immunoprecipitated with A11 antibodies

In the soluble fraction immunoprecipitated with A11 antibodies, binding Aβ in its oligomeric forms no Aβ signal can be detected in any of the mouse models, no significant difference is seen between them (see figure 14).

A)

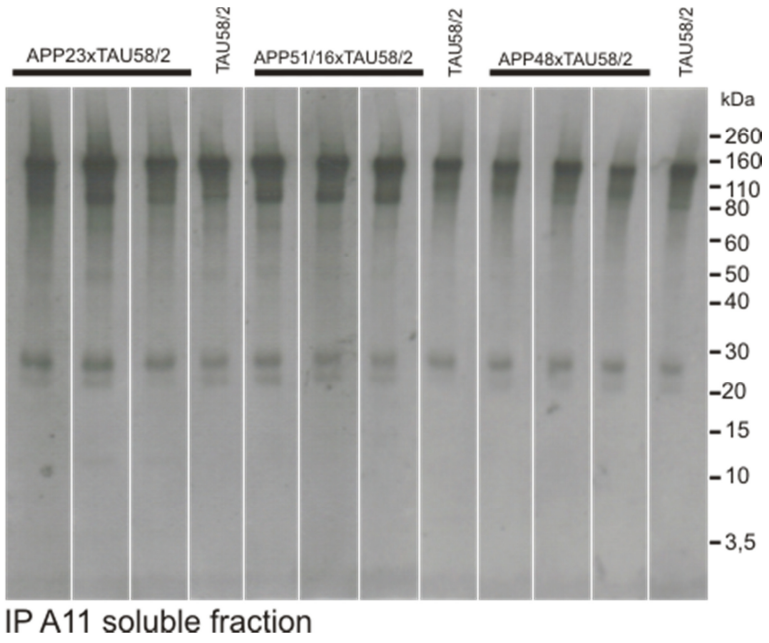

B)

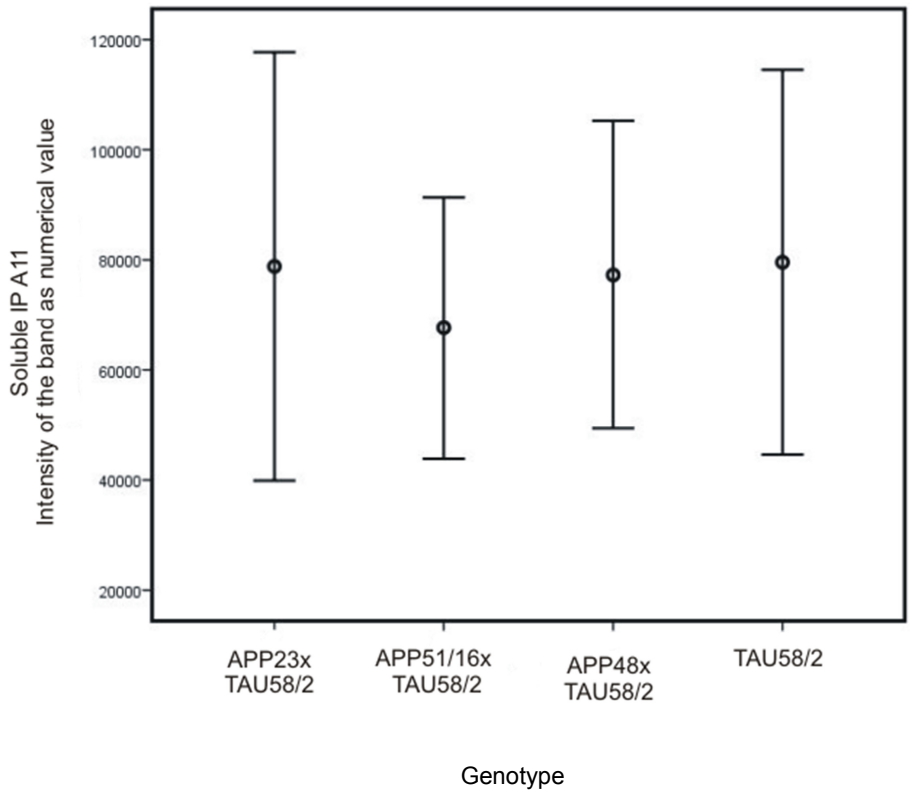

Figure 14: A) Western blot analysis of Aβ in the IPA11 soluble fraction of the different mouse models. For detection of Aβ the 6E10 antibody was used. Aβ occurs as 4kDa molecular weight band. B) Kruskal Wallis test with Dunn-Bonferroni post-hoc test: n = 6 for each group, mean and standard errors are presented. No significant difference between the different mouse models can be detected.

Aβ in the soluble fraction immunoprecipitated with B10 antibodies

In the soluble fraction immunoprecipitated with B10 antibodies, binding fibrillary and protofibrillary Aβ, again no significant Aβ signal can be seen in any of the mouse models (see figure 15). Although in some APP23xTAU58/2 mice weakly stained Aβ bands are visible, no significant difference compared to the other mouse lines can be determined (see figure 15).

A)

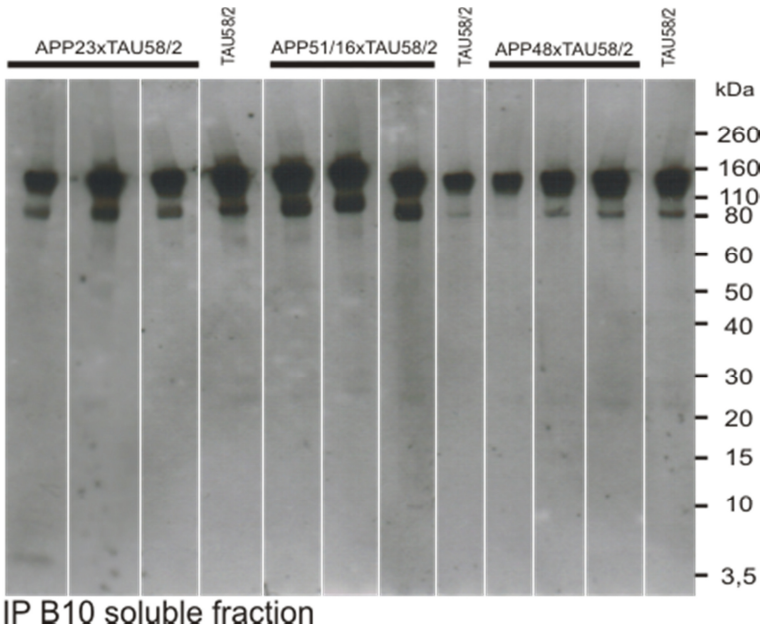

B)

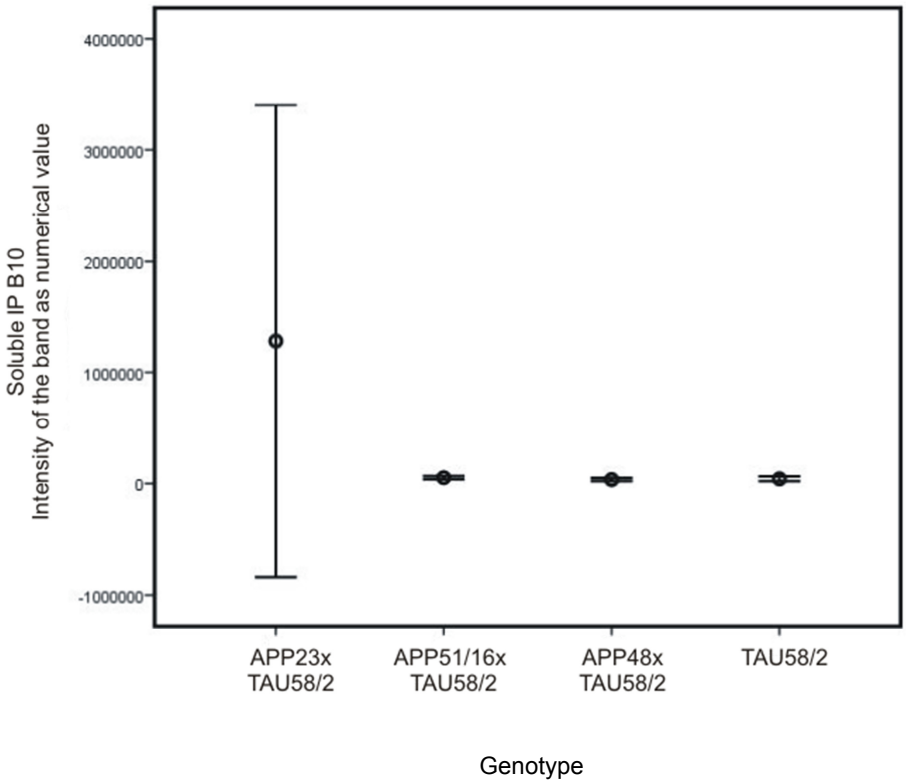

Figure 15: A) Western blot analysis of Aβ in the IPB10 soluble fraction of the different mouse models. For detection of Aβ the 6E10 antibody was used. Aβ occurs as 4kDa molecular weight band. B) Kruskal Wallis test with Dunn-Bonferroni post-hoc test: n = 6 for each group, mean and standard errors are presented. No significant difference between the different mouse models can be detected.

Aβ in the dispersible fraction

In the dispersible fraction, Western blot analyses of Aβ detected with the 6E10 antibody reveal highest levels of Aβ in APP23xTAU58/2 mice. Anyway, the difference is statistically significant only in comparison to TAU58/2 mice (Kruskal Wallis test with Dunn-Bonferroni post-hoc test, z=4,205 p=0,0001; APP23xTAU58/2 n=6, TAU58/2 n=6) (see figure 16). Between the other mouse models no significant differences can be seen.

A)

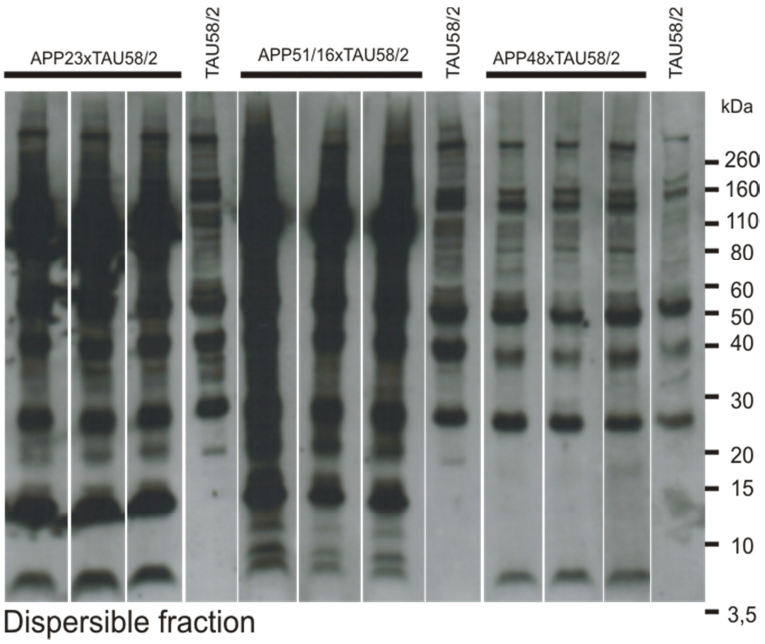

B)

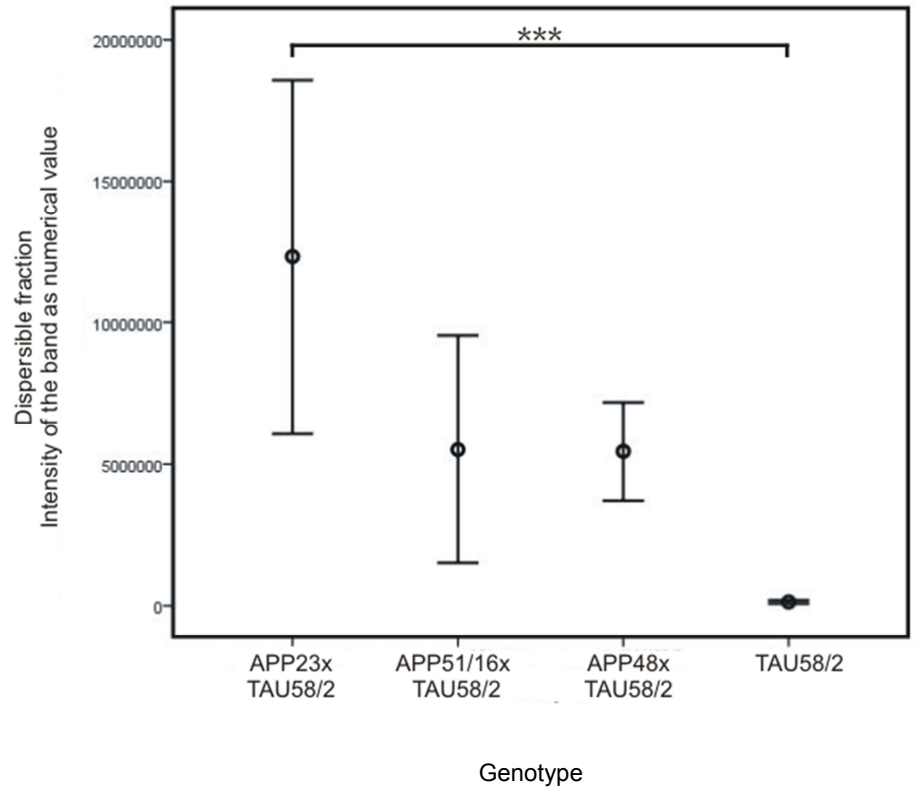

Figure 16: A) Western blot analysis of Aβ in the dispersible fraction of the different mouse models. For detection of Aβ the 6E10 antibody was used. Aβ occurs as 4kDa molecular weight band. B) Kruskal Wallis test with Dunn-Bonferroni post-hoc test: *** $p < 0.001$; $n = 6$ for each group, mean and standard errors are presented. APP23xTAU58/2 show a significant stronger signal than TAU58/2 mice.

Aβ in the dispersible fraction immunoprecipitated with A11 antibodies

In the dispersible fraction immunoprecipitated with A11 antibodies APP23xTAU58/2 (Kruskal Wallis test with Dunn-Bonferroni post-hoc test, z=4,287, p=0,0001; TAU58/2 n=6, APP23xTAU58/2 n=6) and APP48xTAU58/2 mice (Kruskal Wallis test with Dunn-Bonferroni post-hoc test, z=2,858, p=0,026; TAU58/2 n=6, APP48xTAU58/2 n=6) show significant higher levels of Aβ than TAU58/2 mice (see figure 17).
APP23xTAU58/2 mice show higher levels of Aβ than APP51/16xTAU58/2 mice. And APP51/16xTAU58/2 mice contain higher amounts of Aβ than APP48xTAU58/2 and TAU58/2 mice. But these differences are not statistically significant (see figure 17).

A)

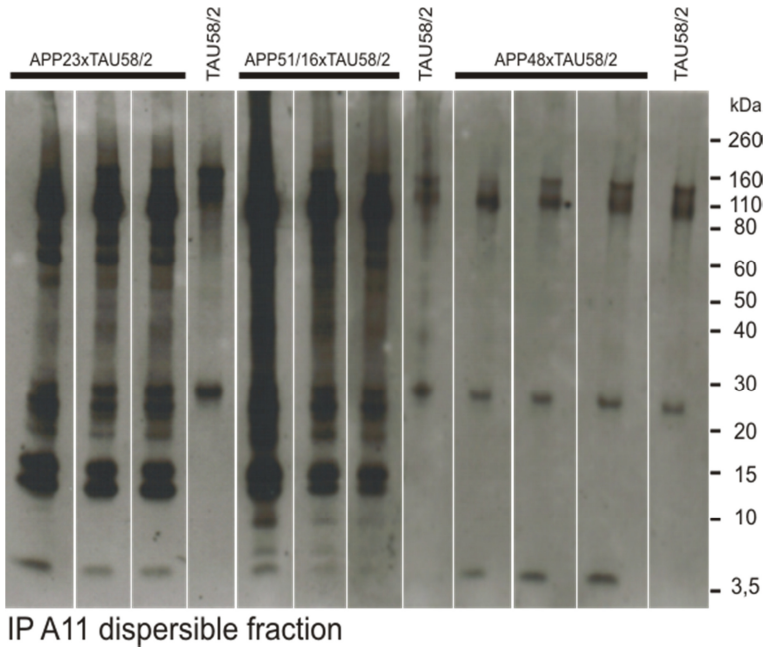

B)

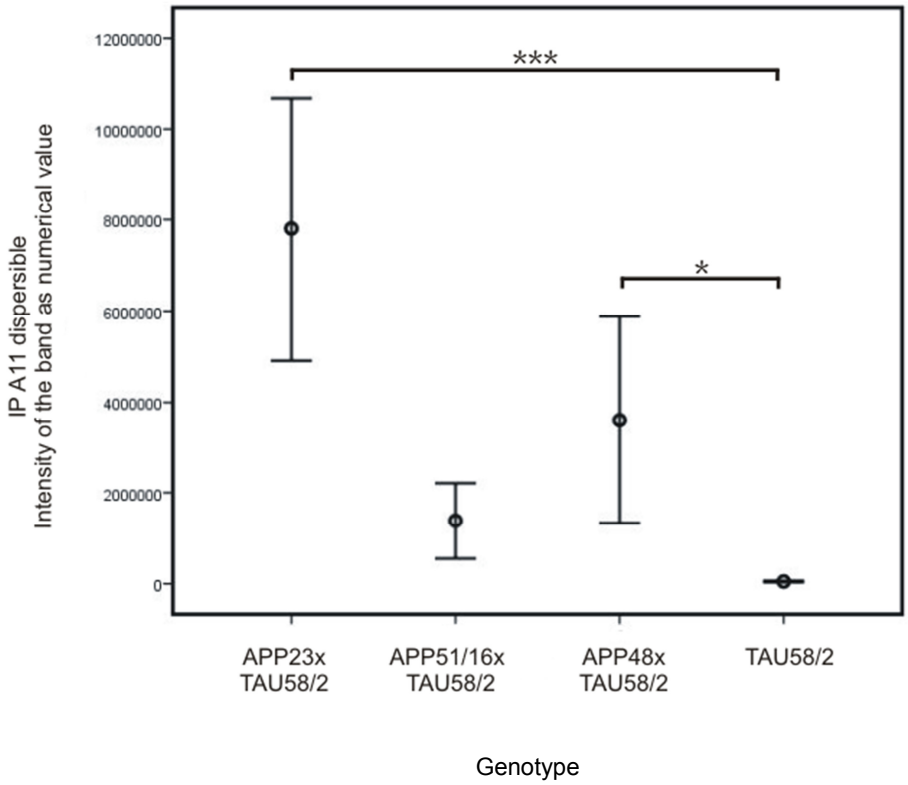

Figure 17: A) Western blot analysis of Aβ in the IPA11 dispersible fraction of the different mouse models. For detection of Aβ the 6E10 antibody was used. Aβ occurs as 4kDa molecular weight band. B) Kruskal Wallis test with Dunn-Bonferroni post-hoc test: * $p < 0.05$; *** $p < 0.001$; n = 6 for each group, mean and standard errors are presented. APP23xTAU58/2 and APP48xTAU58/2 mice show significant stronger signals than TAU58/2 mice.

Aβ in the dispersible fraction immunoprecipitated with B10 antibodies

Also in the dispersible fraction immunoprecipitated with B10 antibodies, APP23xTAU58/2 mice reveal the highest content of Aβ. APP23xTAU58/2 mice here show stronger Aβ bands compared to APP51/16xTAU58/2 (Kruskal Wallis test with Dunn-Bonferroni post-hoc test, z=2,899, p=0,022; APP23xTAU58/2 n=6, APP51/16TAU58/2 n=6) and TAU58/2 mice (Kruskal Wallis test with Dunn-Bonferroni post-hoc test, z=4,368, p=0,0001; APP23xTAU58/2 n=6, TAU58/2 n=6) (see figure 18). In comparison to APP48xTAU58/2 mice no statistically relevant difference is seen. APP48xTAU58/2 mice show significant stronger bands for Aβ compared to TAU58/2 mice (Kruskal Wallis test with Dunn-Bonferroni post-hoc test, z=2,98, p=0,017; APP48xTAU58/2 n=6, TAU58/2 n=6) (see figure 18). In samples of TAU58/2 mice no Aβ can be detected.

A)

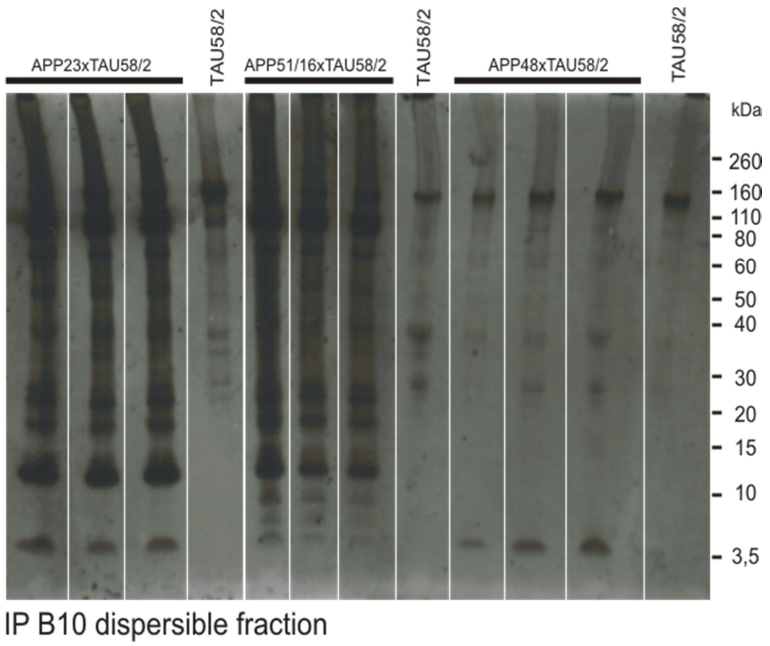

B)

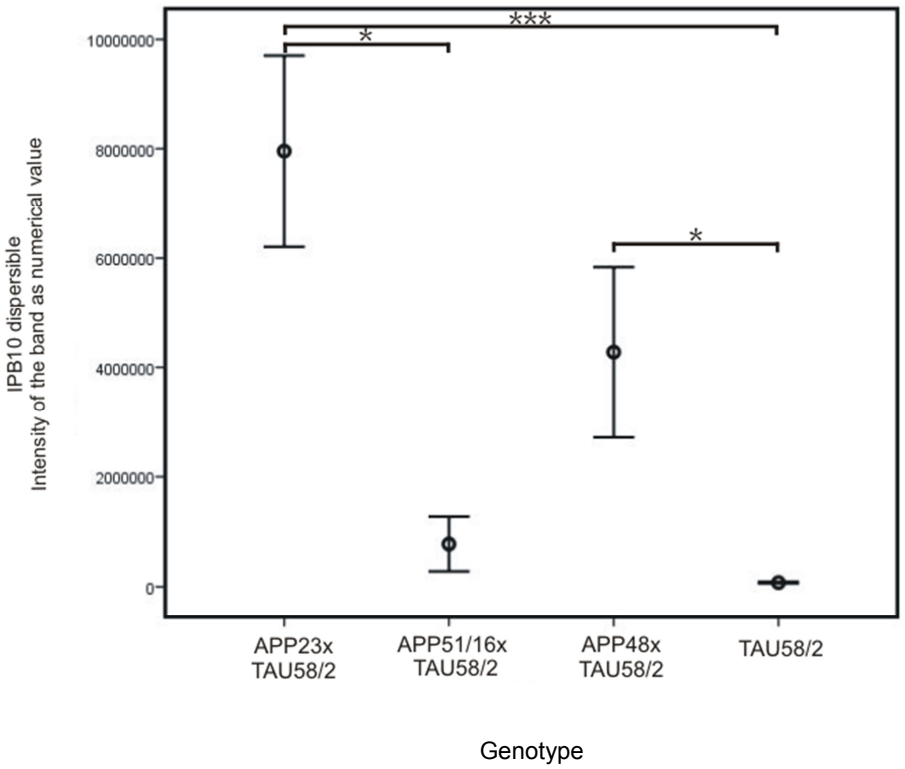

Figure 18: A) Western blot analysis of Aβ in the IPB10 dispersible fraction of the different mouse models. For detection of Aβ the 6E10 antibody was used. Aβ occurs as 4kDa molecular weight band. B) Kruskal Wallis test with Dunn-Bonferroni post-hoc test: * $p < 0.05$; *** $p < 0.001$; n = 6 for each group, mean and standard errors are presented. APP23xTAU58/2 mice show significant stronger signals than APP51/16xTAU58/2, and TAU58/2 mice. APP48xTAU58/2 mice present with significant stronger signals than TAU58/2 mice.

Aβ in the SDS soluble fraction

Western blot analyses of the SDS soluble fraction stained with the 6E10 antibody show similar levels of membrane-associated Aβ in APP23xTAU58/2, APP51/16xTAU58/2 and APP48xTAU58/2 mice. Compared to the TAU58/2 mice, APP23xTAU58/2 mice show significantly stronger Aβ signals (Kruskal Wallis test with Dunn-Bonferroni post-hoc test, z=3,021, p=0,015; APP23xTAU58/2 n=6, TAU58/2/2 n=6) (see figure 19).
Also APP51/16xTAU58/2 (Kruskal Wallis test with Dunn-Bonferroni post-hoc test, z=2,939, p=0,02; APP51/16xTAU58/2 n=6, TAU58/2 n=6) and APP48xTAU58/2 (Kruskal Wallis test with Dunn-Bonferroni post-hoc test, z=2,858, p=0,026; APP48xTAU58/2 n=6, TAU58/2 n=6) mice contain more Aβ than TAU58/2 mice in the SDS soluble fraction (see figure 19).

A)

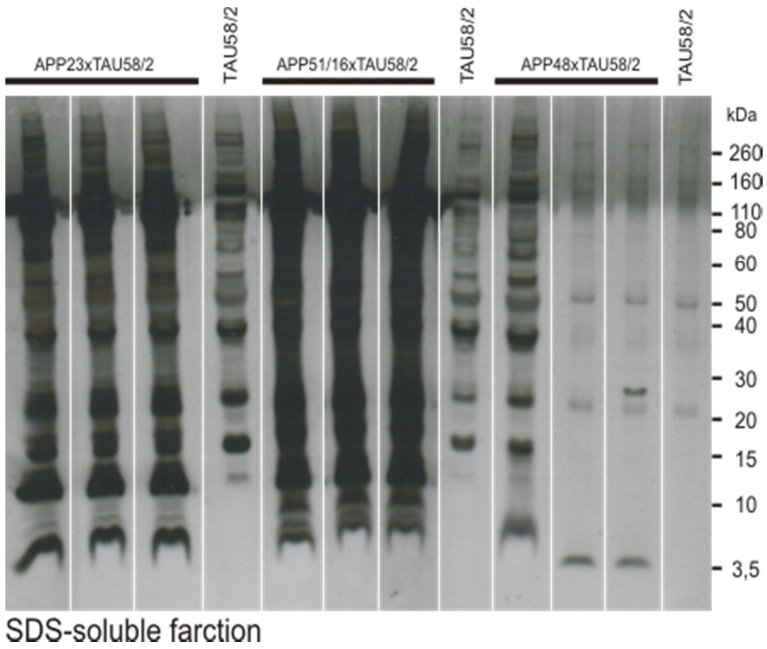

B)

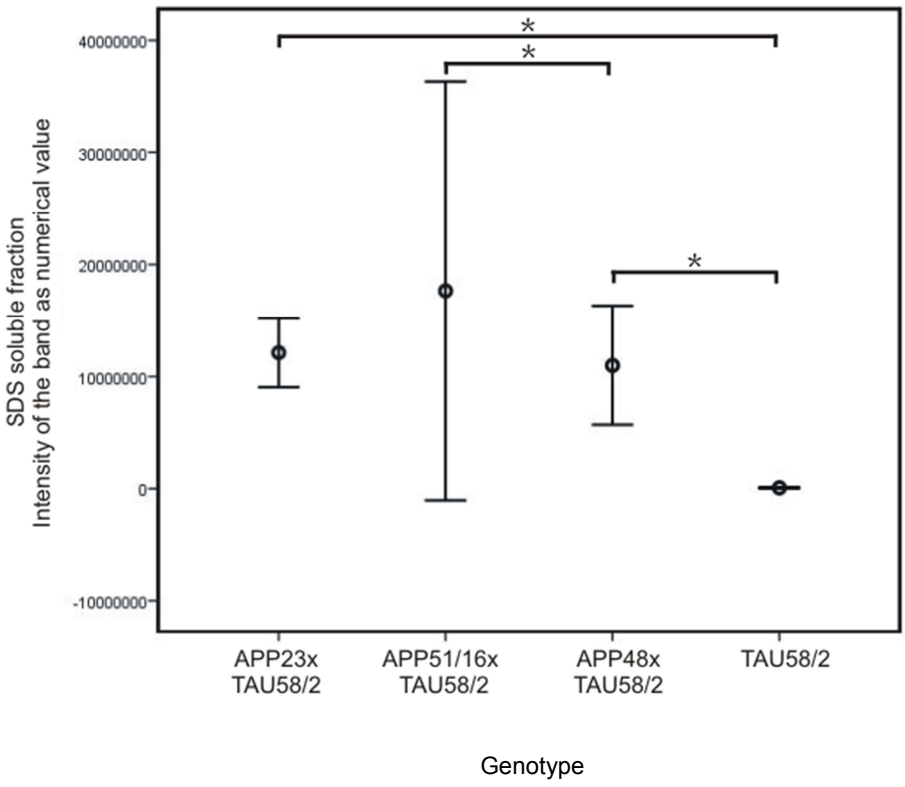

Figure 19: A) Western blot analysis of Aβ in the SDS soluble (membrane-associated) fraction of the different mouse models. For detection of Aβ the 6E10 antibody was used. Aβ occurs as 4kDa molecular weight band. B) Kruskal Wallis test with Dunn-Bonferroni post-hoc test: * $p < 0.05$; n = 6 for each group, mean and standard errors are presented. APP23xTAU58/2 and APP48xTAU58/2 mice show significant stronger signals than TAU58/2 mice, APP51/16xTAU58/2 show stronger signals than APP48xTAU58/2 mice.

Aβ in the formic acid soluble fraction

Western blot analyses with the 6E10 antibody of the formic acid soluble fraction show stronger Aβ signals in APP48xTAU58/2 mice compared to APP51/16xTAU58/2 (Kruskal Wallis test with Dunn-Bonferroni post-hoc test, z=-2,776, p=0,033; APP48xTAU58/2 n=6, APP51/16TAU58/2 n=6) and TAU58/2 mice (Kruskal Wallis test with Dunn-Bonferroni post-hoc test, z=4,246, p=0,0001; APP48xTAU58/2 n=6, TAU58/2 n=6) (see figure 20). APP23xTAU58/2xTAU58/2 mice show little stronger Aβ signals than the APP51/16xTAU58/2 mice, in the formic acid soluble fraction but the difference is not significant. Compared to APP48xTAU58/2 mice, the APP23xTAU58/2 mice present with little lower Aβ signals in the same fraction. But again this difference is not significant. In comparison to TAU58/2 mice, APP23xTAU58/2 mice show significantly higher levels of Aβ in the formic acid soluble fraction (Kruskal Wallis test with Dunn-Bonferroni post-hoc test, z=3,103, p=0,012 APP23xTAU58/2 n=6, TAU58/2 n=6) (see figure 20).

A)

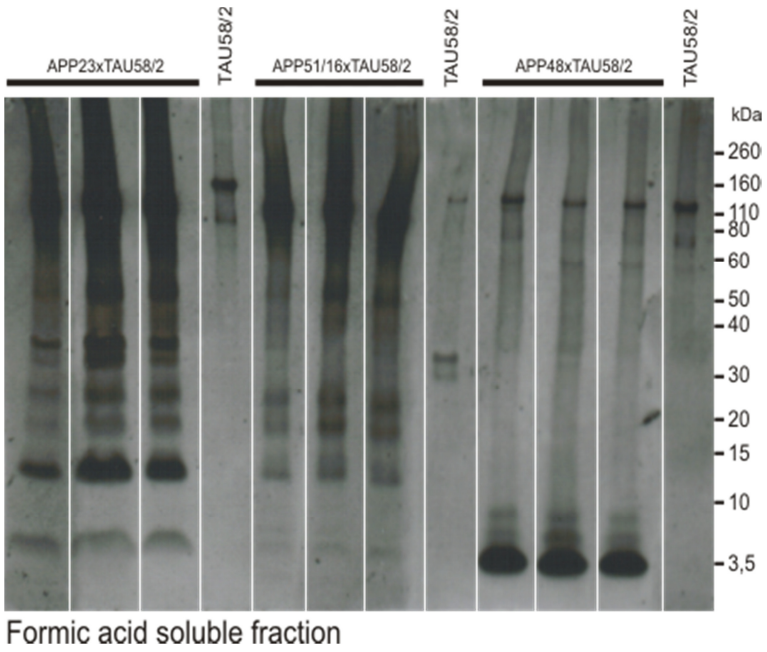

B)

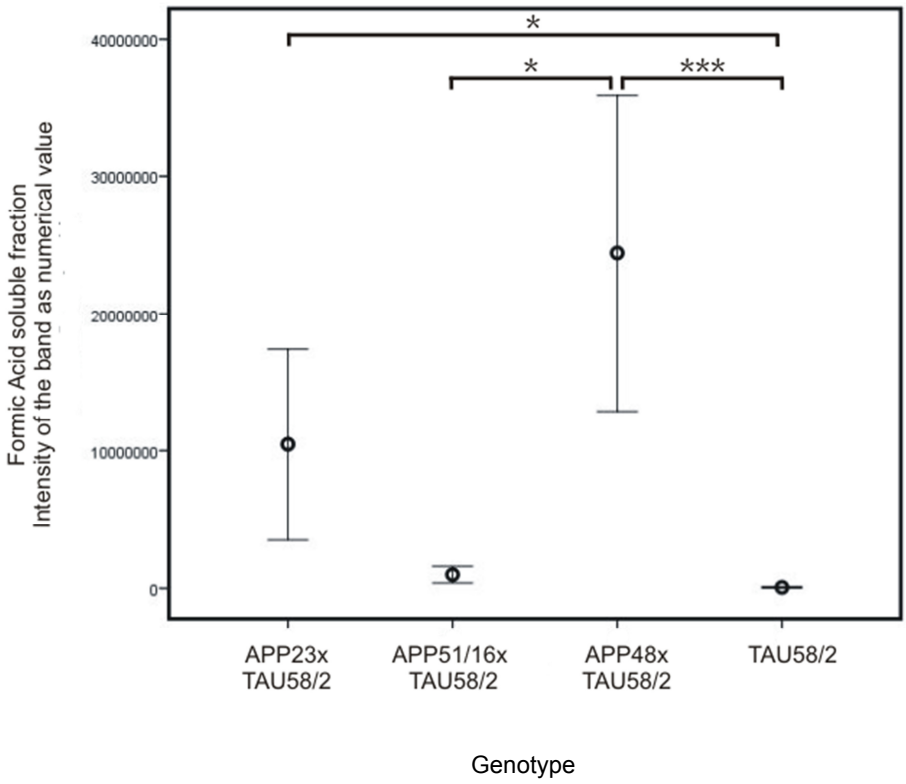

Figure 20: A) Western blot analysis of Aβ in the formic acid soluble (plaque-associated) fraction of the different mouse models. For detection of Aβ the 6E10 antibody was used. Aβ occurs as 4kDa molecular weight band. B) Kruskal Wallis test with Dunn-Bonferroni post-hoc test: * $p < 0.05$; *** $p < 0.001$; n = 6 for each group, mean and standard errors are presented. APP23xTAU58/2 and APP48xTAU58/2 mice show significant stronger signals than TAU58/2 mice. APP48xTAU58/2 mice show stronger signals than APP51/16xTAU58/2 mice.

3.4 Biochemical determination of the tau content in the different mouse models

A total of 28 different samples were analyzed with the MSD® MULTI-SPOT Phospho (Thr231)/Total TAU Assay. APP single transgenic mice serve as control group. All the mouse lines (APP23xTAU58/2, n=4; APP51/16xTAU58/2, n=6; APP48xTAU58/2, n=6; TAU58/2, n=6; APP23, n=2; APP51/16, n=2; APP48, n=2) show similar amounts of phospho tau. No significant differences are seen among the different mouse models (see Figure 21).

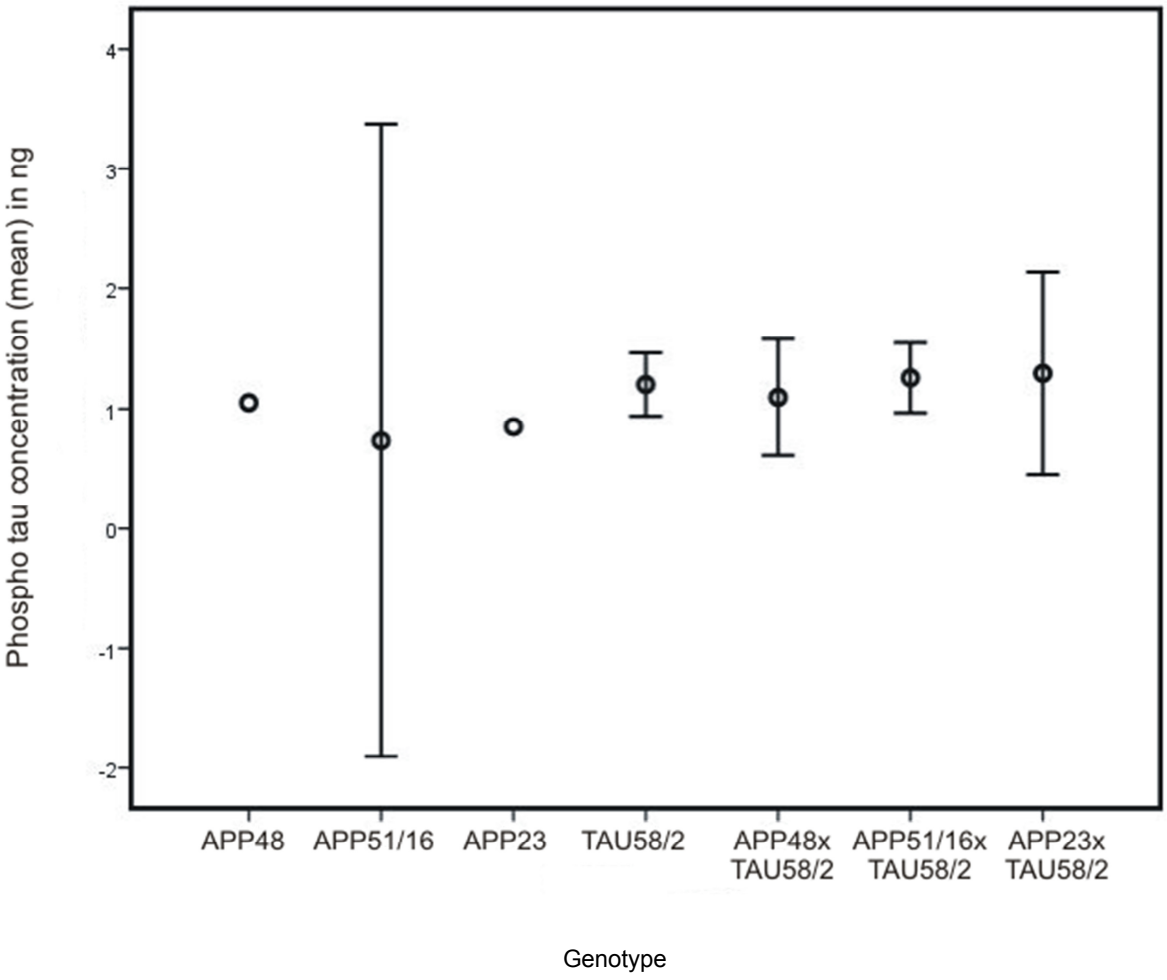

Figure 21: MSD® MULTI-SPOT Phospho (Thr231)/Total TAU Assay. Shown are the results of the phospho tau assay. (Kruskal Wallis test with Dunn-Bonferroni post-hoc test: APP48 n=1, APP51/16 n=2, APP23 n=1, TAU58/2 n=6, APP48xTAU58/2 n = 6, APP51/16xTAU58/2 n=6, APP23xTAU58/2 n=4; for each group, mean and standard errors are presented). No significant difference between the different mouse models can be detected.

In total tau ELISA higher levels of total tau can be seen in the TAU58/2 and APP23xTAU58/2, APP51/16xTAU58/2 and APP48xTAU58/2 double transgenic mice in comparison to APP23, APP51/16 and APP48 mice. Among those mice bearing a tau transgene no significant differences can be detected. There is significantly less total tau in APP48 mice compared to TAU58/2 (Kruskal Wallis test with Dunn-Bonferroni post-hoc test, z=-2,263, p=0,024; APP48 n=2, TAU58/2 n=6) and APP48xTAU58/2 (Kruskal Wallis test with Dunn-Bonferroni post-hoc test, z=-1,980, p=0,048; APP48 n=2, APP48xTAU58/2 n=6). APP51/16 mice present with significant lower amount of total tau in comparison to TAU58/2 mice (Kruskal Wallis test with Dunn-Bonferroni post-hoc test, z=-2,002, p=0,045; APP51/16 n=1, TAU58/2 n=6). APP23 mice show a significant lower content of total tau compared to TAU58/2 (Kruskal Wallis test with Dunn-Bonferroni post-hoc test, z=-2,649, p=0,008; APP23 n=2, TAU58/2 n=6) and APP48xTAU58/2 mice (Kruskal Wallis test with Dunn-Bonferroni post-hoc test, z=2,366, p=0,018; APP23 n=2, APP48xTAU58/2 n=6) (see figure 22).

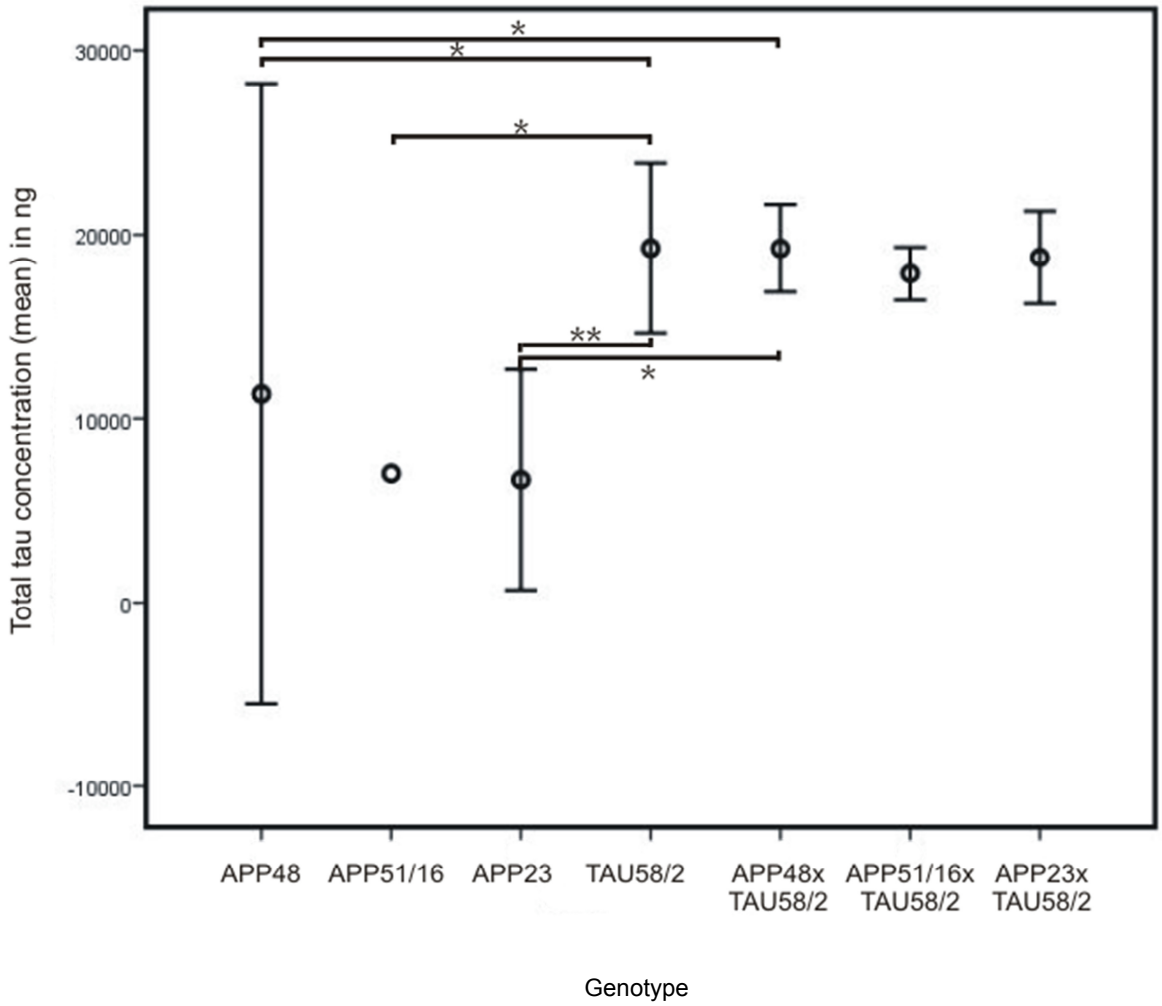

Figure 22: MSD® MULTI-SPOT Phospho (Thr231)/Total TAU Assay. Shown are the results of the total tau assay. (Kruskal Wallis test with Dunn-Bonferroni post-hoc test: * $p < 0.05$; ** $p < 0.01$; APP48 n=2, APP51/16 n=2, APP23 n=2, TAU58/2 n=6, APP48xTAU58/2 n = 6, APP51/16xTAU58/2 n=6, APP23xTAU58/2 n=4; for each group, mean and standard errors are presented). APP single transgenic mice show lower concentrations of total tau than the double transgenic and TAU58/2 mice.

4. Discussion

The aims of this study were to find out more about how Aβ and tau protein interact in regard to the generation of AD-related tau and Aβ pathology. Therefore, I studied three different APP and tau double transgenic mouse models with three different APP/Aβ transgenes, each crossed with a relatively novel mouse model for tau pathology, the TAU58/2 mouse.

Here, I found that APP23xTAU58/2 mice, a mouse model that produces large amounts of Aβ crossed with TAU58/2 mice, show the highest amount of hyperphosphorylated and aggregated tau protein detected with immunohistochemistry when compared to APP51/16xTAU58/2 and APP48xTAU58/2 mice. Interestingly, using ELISA no such differences between the different double transgenic mouse models were seen when measuring the amount of phosphorylated tau and total tau in the brain. This might indicate that Aβ as it arises in APP23xTAU58/2 mice could aggravate the aggregation of hyperphosphorylated tau. The crucial Aβ species triggering the accumulation of pathological neuronal tau aggregates seems to be the soluble Aβ. Moreover, this effect most likely depends on the formation of Aβ via APP processing because non APP-related artificially produced intracellular Aβ in APP48 mice (here, Aβ is inserted into the endoplasmic reticulum after cleavage from a rat proencephalin signal peptide) does not have an influence on tau aggregation. The fact that pretangle-/ or neurofibrillary tangle-like tau pathology is not seen in APP23 mice without transgenic mutant tau protein expression(Sturchler-Pierrat et al. 1997), argues in favor of the hypothesis that the presence of “aggregation prone” tau protein is essential for Aβ to exaggerate tau pathology and, finally, leading to the formation of NFTs.

Furthermore, this study confirms that the TAU58/2 mouse model is a promising mouse model for studying tau pathology. TAU58/2 mice do actually produce more tau than tau-non expressing mouse models as we can see in the total tau measures determined by ELISA and they show Gallyas-stained neurofibrillary tangles as well as positive neurons in RD4 staining, although the levels of phosphorylated tau protein measured by ELISA did not significantly increase in comparison to other mouse models, harboring no tau transgene.

4.1 Aβ accelerates tau aggregation in a dose dependent manner

The first point to be discussed in detail is the finding that Aβ appears to exaggerate the aggregation of tau possibly by cross-seeding. The results of the immunohistochemical staining with the AT8 antibody and the following assessment of the percentage of AT8-positive neurons show that APP23xTAU58/2 mice present with the highest percentages of neurons containing hyperphosphorylated tau protein. However, ELISA analyses exhibit no difference in the concentration of phosphorylated tau among the different mouse models. In the immunohistochemical staining with the AT8 antibody, aggregates or accumulations of hyperphosphorylated tau protein in the neurons forming pretangles or neurofibrillary tangles can be visualized. These results of the neuronal cell count in AT8 staining and the ELISA analyses indicate that not the total concentration of the phosphorylated tau protein differs among the mouse models but the accumulation of aggregated, phosphorylated tau protein in pretangles and neurofibrillary tangles does. This indicates, that Aβ as it is found in APP23xTAU58/2 mice might accelerate the aggregation of tau protein in distinct neurons and hence promote neurofibrillary tangle formation. As immunohistochemical staining reveals that in six months old APP23xTAU58/2 mice, Aβ plaques were absent in most animals (only one animal showed single plaques), Aβ plaques seem not to be a relevant factor for triggering tau pathology. To determine in which biochemical form Aβ is critical for exaggerating tau pathology, Western blot analyzes were performed. When focusing on differences between APP23xTAU58/2 and the other examined mouse models it becomes evident that APP23xTAU58/2 mice show high amounts of soluble Aβ. This difference is statistically significant compared to APP48xTAU58/2 and TAU58/2 mice. In comparison to APP51/16xTAU58/2 mice no statistically relevant difference can be seen, although also here the level of Aβ is higher in the APP23xTAU58/2 mice. These results indicate that soluble Aβ is likely crucial for the interplay between Aβ and tau pathology and that soluble Aβ might trigger tau pathology in AD. One possibility for an interaction between Aβand tau is cross-seeding. The fact that we do not see such amounts of tau pathology in APP51/16xTAU58/2 as in APP23xTAU58/2 transgenic mice in the immunohistochemical staining with AT8 antibody may indicate that cross-seeding of tau and Aβ takes place in a dose dependent manner. APP48xTAU58/2 mice only produce little soluble Aβ, which

again shows that the effect of soluble Aβ on tau pathology seems to be relevant and dose dependent. Although APP51/16xTAU58/2 mice also generate soluble Aβ they do not show as many AT8 positive neurons as APP23xTAU58/2 mice, but more than APP48xTAU58/2 mice. Although a statistical difference between the amount of soluble Aβ between APP23xTAU58/2 and APP51/16xTAU5872 mice cannot be seen, the tendency is obvious, that APP23xTAU58/2 mice contain more soluble Aβ. As no Aβ bands are seen in the soluble fractions immunoprecipitated with A11 and B10 antibodies in all of the mouse models it is very likely that neither Aβ oligomers nor Aβ fibrils are crucial for exaggerating tau pathology. It has to be assumed, that instead monomeric Aβ or low molecular weight oligomers, which were not immunoprecipitated with A11 antibodies might represent the crucial entity for the interaction between Aβ and tau. APP23xTAU58/2 mice also show high amounts of dispersible Aβ. Especially in the dispersible fractions immunoprecipitated with B10 antibodies, APP23xTAU58/2 mice show high levels of Aβ. Anyhow, high levels of Aβ in the dispersible fraction are also seen in APP48xTAU58/2 mice. These mice contain even more Aβ in this fraction than APP51/16xTAU58/2 mice but APP51/16xTAU58/2 mice show more neurons containing hyperphosphorylated tau in the AT8 staining than APP48xTAU58/2 mice. This argues against dispersible Aβ being relevant for formation of neurofibrillary tangles. Taken together, the soluble Aβ more likely induces cross-seeding with tau, whereas dispersible Aβ appears less obviously involved in this process.

To provide further arguments in favor of a cross-seeding process I will now discuss my findings in the light of the seeding process in more detail. The seeding-nucleation-polymerization model explains how amyloid aggregates develop. A seeding nucleus is formed by oligomeric misfolded proteins inducing a quick and exponential misfolding of normally folded monomeric proteins. The newly aggregated proteins also act as new seeds promoting further polymerization and aggregation (Jarrett u. Lansbury 1993). Several studies have shown that tau itself is able to propagate tau pathology in a prion-like spreading through functionally connected brain regions (Clavaguera et al. 2009; Clavaguera et al. 2013; Goedert et al. 2010; Iba et al. 2013). It has also been described in different studies that Aβ can promote tau pathology by cross-seeding in vitro and in vivo (RW.ERROR - Unable to find reference:123; Umeda et al. 2014; Vasconcelos et al. 2016). Cross-seeding means that aggregates of misfolded proteins are capable to cause polymerization of a second protein. For example it was discovered that the injection of Aβ

fibrils in brains of tau mutant P301L mice lead to a fivefold increased number of NFTs (Gotz et al. 2001). Even the injection of human tau in APP mutant mouse brains resulted in the formation of NFTs, even if the mouse itself does not bear a tauopathy-related mutation (Umeda et al. 2014). By crossbreeding APP transgenic mice with tau transgenic mice increased NFT formation was reported (Lewis et al. 2001). Another argument for the cross-seeding connection between Aβ and tau pathology gives a study, which shows that in mouse models developing Aβ plaques and NFTs immunotherapy against Aβ not only leads to a reduction of Aβ plaques but also to a decrease in tau pathology (Oddo et al. 2004). Similar findings were made by Vasconselos et al. showing that pre-aggregated Aβ causes fibrillization of tau in vitro and in vivo (RW.ERROR - Unable to find reference:123; Vasconcelos et al. 2016) . These are only examples for several studies which all point to the conclusion that Aβ actually is capable of aggravating and accelerating tau pathology. In most of these studies Aβ is added as a seed either in vitro to cells or it is injected in vivo into the brain. Most of these studies share the disadvantage that Aβ was imported into a system from outside. In contrast to this, we here see the effects of the proteins on one another when they are endogenously produced in one animal; nothing has to be added from outside, which provides the possibility to see the effects of Aβ and tau when endogenously produced and accumulating in one animal. Thus, these double transgenic mouse models provide the opportunity to study the effects of Aβ produced APP-dependent and APP-independent as well as tau when they arise in the brain at the same time under different transgenic (artificial) conditions, which cannot be tested in the event that Aβ is added by injection to already preexisting tau pathology.

As such one could assume not Aβ itself might be responsible for the increase in tau pathology but the overexpression of APP. If this would be the case, there should be equal levels of tau pathology in APP51/16xTAU58/2 and APP23xTAU58/2 mice because both mouse lines, APP23 and APP51/16 produce similar levels of APP (Rabe et al. 2011). However, in APP51/16xTAU58/2 mice the immunohistochemical staining with the AT8 antibody shows lower numbers of AT8 positive neurons than in APP23xTAU58/2 mice. If only the overexpression of APP would be sufficient to increase tau pathology, this effect should also be seen in APP51/16xTAU58/2 mice.

Taken together, these circumstances lead to the conclusion that cross-seeding of Aβ and tau is one option to explain the exaggeration of tau pathology in APP23xTAU58/2 mice in comparison to the other studied mouse models here. Not only the presence of soluble Aβ is crucial but also a specific concentration that drives the tau pathology in a dose dependent manner and that Aβ is critical for the aggravation of tau pathology. Nevertheless, APP also plays an important role for the interplay between Aβ and tau which shall be discussed next.

4.2 The role of APP-derived Aβ processing for its interaction with tau

A further finding is that the process of cross-seeding of Aβ and tau is only seen in mouse lines, where Aβ is produced by the cleavage of APP. In APP48xTAU58/2 mice where Aβ is generated independently from APP no increase of tau pathology was detected. The examination of this mouse model further indicates that extracellular Aβ may be necessary for cross-seeding of tau by Aβ or exaggerating tau pathology driven by another mechanism, because APP48xTAU58/2 mice only express intracellular Aβ in the endoplasmic reticulum and the Golgi apparatus (Abramowski et al. 2012). Otherwise, it remains unclear whether the intracellular Aβ in APP48xTAU58/2 mice gets in touch with intracellular located tau protein because of its generation in the endoplasmic reticulum. Although immunofluorescence double labelling shows intracellular Aβ colocalized with tau in the same neurons in APP48xTAU58/2 mice, this colabelling has no effect on exaggeration of tau pathology. Other studies which have shown, that Aβ accelerates tau aggregation when it is added as seeds to cells (Vasconcelos et al. 2016) or injected into brains (Gotz et al. 2001), also support the idea that the extracellular localization of Aβ might play an important role for the effects of cross-seeding with tau to form neurofibrillary tangles. A disadvantage of the APP48 mouse model is that it is a very artificial model of Aβ pathology. The way Aβ is generated is different from the physiological generation in the human brain. However, by doing so this mouse model offers the chance to study the effects of Aβ in intracellular compartments.
The discussed points until now sum up the prerequisites, which are required for Aβ to exaggerate tau pathology. In addition, there also seem to be conditions for tau, which

have to be fulfilled to enable Aβ is able of triggering tau aggregation. This shall be illustrated next.

4.3 "Aggregation prone" tau protein is a prerequisite for Aβ to exaggerate tau pathology

In immunohistochemical staining of APP23 mice´s brain sections with the AT8 antibody, only in older animals (12 months of age) some neuritic plaques were detected (Sturchler-Pierrat et al. 1997). No pretangles or neurofibrillary tangles were described as detected here in APP23xTAU58/2 mice. Immunoprecipitation with subsequent Western blot analyses of APP23 revealed high levels of fibrillary and oligomeric Aβ in the dispersible brain fraction of these animals, which were significantly higher than in APP51/16 mice (Rijal Upadhaya et al. 2012). Moreover, at the age of 5-6 months only a subset of the APP23 mice shows plaques and none of the APP51/16 mice does (Capetillo-Zarate et al. 2006; Rijal Upadhaya et al. 2012). As such, APP23 transgenic mice show a similar pattern of Aβ than APP23xTAU58/2 mice in Western blot analyzes and Aβ plaque pathology but they do not show aggravated tau pathology like APP23xTAU58/2 mice. The fact that this finding is not seen in APP23 mice without transgenic mutant tau protein expression leads to the conclusion that the presence of "aggregation prone" tau protein is essential for Aβ to stimulate the formation of NFTs.

These findings are coherent with my findings in APP51/16xTAU58/2 mice and with results of other groups (Braak et al. 2011; Spires-Jones et al. 2017) that there is an interplay between Aβ and tau. It is known that the pure existence of Aβ aggregates does not lead to cognitive decline. In human autopsy brains Aβ pathology can be seen already in young individuals. First Aβ aggregations might occur at the age of 11-20 years and increases then with age (Braak et al. 2011; Spires-Jones et al. 2017).
Mutations causing familiar forms of AD do not only lead to Aβ aggregations but also tau pathology can be seen (Spires-Jones et al. 2017). This indicates that Aβ can trigger tau pathology and may on the first glance argue in favor for the amyloid cascade hypothesis that development of tau pathology is a downstream effect in relation to Aβ pathology.

However, there are several tauopathies causing neurological symptoms (for example Pick´s disease) which present only with tau but not with Aβ pathology (Dickson 1998). Moreover, tau pathology is detectable already early in human brains, even in individuals without clinical symptoms of a neurological disease or Aβ deposition. At the age of 40 years most humans show tau pathology in the brainstem (Spires-Jones et al. 2017; Braak et al. 2011). It is still a matter of debate if these findings are associated with AD or if they are independent from AD (Crary 2016; Duyckaerts et al. 2015; Jellinger et al. 2015). But the pathology in this stage does not exceed transentorhinal and limbic cortex (Braak u. Braak 1991; Braak u. Del Tredici 2011; Spires-Jones et al. 2017). The widest spreading of tau pathology through the brain (Braak Stages V/VI) is only seen if there is also Aβ pathology. Tau pathology propagates in early stages into other brain regions than Aβ pathology in early stages. This may also be caused by seeding along functionally connected brain regions. It has been shown that injection of Aβ in APP and PS1 transgenic mice led to an aggravation of tau pathology not only at the place where Aβ was injected into the brain but also in functionally connected brain regions (Bolmont et al. 2007; Gotz et al. 2001).

Taken together, findings from other groups in context of my results lead to the conclusion, that the amyloid-cascade hypothesis has to be modified. The amyloid-cascade hypothesis postulates that Aβ initiates tau pathology in AD. If this would be the case, all APP transgenic mouse models should also generate tau pathology, which they do not. The results of my study show, that the existence of “aggregation-prone” tau protein is a prerequisite for Aβ to exaggerate tau pathology. Hence, it is likely that Aβ alone is not capable of initiating all pathological changes in AD, but rather of exaggerating NFT formation in the event of preexisting neuronal tau pathology.

This study helps to clarify, which types of Aβ are able to exaggerate tau pathology and which prerequisites are necessary for this interplay. All these findings which support to the assumption of an interaction of Aβ and tau pathology raise the question where this interaction takes place.

4.4 Potential site of interaction between Aβ and tau

As Aβ accumulates in the extracellular space and hyperphosphorylated tau protein accumulates intraneuronally, possible places of interaction are the synapses. It has been shown that tau is released at synapses in AD (Sokolow et al. 2015). Arguments for this hypothesis provides a study, which showed that application of Aβ to cultured neurons led to a loss of synapses and an increased phosphorylation of tau in the dendrites (Zempel et al. 2010). Furthermore, synapses are an important target for pathological mechanisms in AD. Dysfunction or even loss of synapses is the strongest anatomical correlate of decreased cognitive functions. Moreover, the synapses provide a link between functionally connected brain regions, which could explain how spreading of tau pathology along such regions happens. Co-occurrence of Aβ and tau at synapses in mouse and human brain was already described by the use of array tomography (Spires-Jones et al. 2017). Furthermore, it was described before that both Aβ and tau can influence synaptic structures and receptors.

Here, co-seeding of synaptically released abnormal tau by Aβ could take place as discussed in detail in 4.1.

Alternatively an indirect way of interaction can be discussed. It is well known that Aβ influences synapses through binding or/ and disruption of NMDA receptors. Aβ negatively regulates the number of NMDA receptors and enhances the internalization of the latter. These events finally lead to a decreased calcium influx into dendritic spines and, thereby, to synaptic spine shrinkage and retraction (Shankar et al. 2007; Snyder et al. 2005). Another mechanism is that fibrillary Aβ binds to cell surface receptor cellular prion protein (PrPc) leading to the activation of Rrc kinase Fyn, which causes phosphorylation of NMDA receptors, and hence, a loss of surface NMDA receptors (Um et al. 2012).

In addition, tau targets Fyn to the spine under physiological conditions. Here, Fyn phosphorylates NMDA receptors leading to excitotoxicity as mentioned earlier by the loss of NMDA receptors (Ittner et al. 2010). If Aβ and hyperphosphorylated tau occur in increased levels more Fyn is targeted to the spine, which heightens the toxic effects of Aβ on NMDA receptors. Studies with APP transgenic mouse models showed that reduction of tau in these animals resulted in reduced susceptibility to excitotoxicity and a decreased early mortality without changes of the Aβ levels (Roberson et al. 2007).

Aβ initially leads to over excitation of NMDA receptors and hence to an elevated localized calcium influx into the cell (Zempel et al. 2010). The increased calcium levels activate the kinases AMPK and PAR-1/MARK which cause tau phosphorylation (Mairet-Coello et al. 2013). It has been proposed that Aβ might activate Fyn and hence accelerates loss of synapses (Yu et al. 2012; Mairet-Coello et al. 2013). These findings show how Aβ can trigger the phosphorylation of tau by activating AMP and PAR-1/MARK kinases. Interestingly tau itself aggravates the toxic effects of Aβ via targeting Fyn. These mechanisms describing how Aβ influences the tau pathology might also play a modulatory role in the process of cross-seeding.

This concept that Aβ influences and exaggerates tau pathology by modulating cell surface receptors or cell membrane structures can also be seen in Guam-disease. This is a neurodegenerative disorder of Chamarro residents of Guam presenting with neurofibrillary tau pathology similar to that seen in AD (Forman et al. 2002; Kovacs 2015; Schwab et al. 1998). Although the exact pathomechanism is not fully clear yet, it is assumed that an overstimulation of NMDA receptors by an environmental neurotoxin leads to the formation of tau pathology. As Aβ is able to stimulate NMDA receptors, an overstimulation of NMDA receptors should also be seen in APP single transgenic mice leading to the formation of neurofibrillary tangles. As we do not see this in APP single transgenic mice, other mechanisms such as the co-seeding mechanism appear to be more likely to explain the interaction between Aβ and tau.

It has been shown, that tau gets secreted at synapses (Sokolow et al. 2015). Here, tau becomes extracellular and might alternatively interact physically-chemically with Aβ. By this direct interaction Aβ might trigger the aggregation of tau protein by cross-seeding. If aggregated tau protein might get internalized at the synapses again, this aggregated tau might lead to further aggregation of tau in the neuron. As tau itself might act as seed in the neuron, smaller amounts of phosphorylated tau protein are necessary to further aggregate.

Probably, both ways how Aβ exaggerates tau pathology take place; a modulation of membrane receptors by Aβ and the direct cross-seeding of Aβ and tau. Both effects may act cumulative.

Taken together, these results may explain a key event in the pathomechanism of AD, explaining the parallel expansion of Aβ and tau pathology in the pathogenesis of AD as

seen in human brain autopsy studies (Thal et al. 2013). The understanding of the pathomechanism in AD is crucial and essential for the discovery and development of new possible therapeutic strategies. The key question, which has now to be answered after the findings of this study is, how to stop the cross-seeding of soluble Aβ and tau and, hence, the progression of AD. This might offer new therapeutic targets to stop the cognitive decline and maybe also improve the cognitive abilities in AD patients. Studies with APP transgenic mouse models have shown that neurological symptoms and even the mortality were regressive when tau was removed (Roberson et al. 2007). By better understanding of the mechanisms of Aβ-tau cross-seeding new therapeutic targets could be found.

4.5 TAU58/2, a relevant animal model for tau pathology

For this study, a relatively new tau transgenic mouse model was used, the TAU58/2 mouse (van Eersel et al. 2015). In this study, it can be confirmed that the TAU58/2 mouse is a relevant animal model for tau pathology that produces significant levels of tau pathology in a highly reproductive manner. As I see it immunohistochemically all the mice, which were crossbred with TAU58/2 mice and of course the TAU58/2 mice itself show obviously positive staining with AT8 antibody. TAU58/2 mice also present with typical neurofibrillary tangles in Gallyas silver staining, which is in line with an earlier description of the mouse model (van Eersel et al. 2015). Furthermore, in immunohistochemical staining with the RD4 antibody we also see positive neurons, as expected in mice carrying the P301S mutation related to the four-repeat tauopathy frontotemporal lobar degeneration, whereas in the staining with the RD3 antibody we do not. ELISA analysis verified that the animals crossbred with TAU58/2 mice and the TAU58/2 mice itself contain clearly higher concentration of total tau protein compared to the animals which do not carry the tau transgene. In ELISA analyses of the concentration of phosphorylated tau protein, no difference was seen to non tau transgenic mice indicating that abnormal phosphorylation is restricted to a few neurons and does not allow the detection of these effects in brain homogenates.

5. Summary

Although Alzheimer´s disease (AD) was first described already in 1907, until today the exact pathomechanisms of the disease are not fully understood. Amyloid β (Aβ) is thought to interact with and influence tau pathology but it is not clear how such an interaction takes place. The aims of this study were to find out more about the influence that different types of Aβ pathologies may have on tau pathology in AD. Therefore, amyloid precursor protein (APP) and tau double transgenic mice were examined. APP23xTAU58/2 mice were selected, because APP23 mice are the only APP transgenic mice presenting with loss of neurons even in the single transgenic APP23 mouse. Harbouring human APP with the Swedish mutation (670/671 KM→NL) they produce significant amounts of Aβ. In APP51/16xTAU58/2 mice human wild type APP is overexpressed, these mice produce less Aβ than APP23xTAU58/2 mice. To see the effects of intracellular Aβ on tau pathology, APP48xTAU58/2 mice were chosen with APP48 mice being known to produce intracellular Aβ.
Tau pathology in the mouse brains was visualised by immunohistochemical stainings with antibodies against abnormal phosphorylated tau protein, 3-repeat and 4-repeat tau protein. APP23xTAU58/2 mice showed more tau pathology than the other mouse models, presenting with higher numbers of neurons containing aggregated, hyperphosphorylated tau protein. Enzyme linked immunosorbent assay
(ELISA) analyses were performed to measure the content of total and phosphorylated tau protein. Here, no difference was seen in the amount of phosphorylated tau among the different mouse models, whereas the mice harbouring the tau transgene showed higher levels of total tau than mice without tau transgene. This showed that APP23xTAU58/2 mice do not differ in the amount of phosphorylated tau from the other APPxTAU58/2 mouse models, but in the neuron specific pathological aggregates and phosphorylation of tau protein as represented by the number of pretangles and neurofibrillary tangles. To clarify, which forms of Aβ might be responsible for exaggerating tau pathology, western blot analyses with the 6E10 antibody raised against Aβ1-17 of different fractions of brain homogenates were performed. Herewith, it was seen, that APP23xTAU58/2 mice show more Aβ in the soluble fraction than the other mouse models. APP51/16xTAU58/2 mice expressing human wildtype APP and producing less Aβ than APP23xTAU58/2 mice exhibit

lower number of neurons containing hyperphosphorylated and aggregated tau protein than APP23xTAU58/2 mice but more than TAU58/2 and APP48xTAU58/2 mice also showed lower levels of soluble Aβ than APP23xTAU58/2 but higher than APP48xTAU58/2 and TAU58/2 mice, indicating that the Aβ induced increase of tau pathology takes place in a dose dependent manner. Western blot analyses of soluble brain fractions after immunoprecipitation for oligomers, protofibrils and fibrils did not show relevant amounts of fibrillary or oligomeric Aβ in none of the mouse models, indicating that the critical Aβ species was associated with monomers or low molecular weight oligomers.

APP23 mice have already been described to show only very little tau pathology. This suggests that a prerequisite for soluble Aβ to aggravate tau pathology is the presence of low levels of abnormal tau protein aggregates for initiating the process of tau pathology. The potential site of interaction of Aβ and tau are the synapses, where tau can be released into the perisynaptic extracellular space where it may interact with extracellular Aβ. Further, Aβ can cause tau phosphorylation by modulating synaptic receptors and activation of kinases. Tau itself supports these mechanisms.

These possible interactions between Aβ and tau at the synapses as well as coseeding effects might represent a key event in the pathogenesis of AD, explaining the parallel expansion of Aβ and tau pathology in the pathogenesis of AD as seen in human brain autopsy studies.

6. References

1. Abramowski D, Rabe S, Upadhaya A R, Reichwald J, Danner S, Staab D, Capetillo-Zarate E, Yamaguchi H, Saido T C, Wiederhold K H, Thal D R, Staufenbiel M: Transgenic expression of intraneuronal Abeta42 but not Abeta40 leads to cellular Abeta lesions, degeneration, and functional impairment without typical Alzheimer's disease pathology. The Journal of neuroscience : the official journal of the Society for Neuroscience, 32: 1273-1283 (2012)

2. Alzheimer A.: Über eine eigenartige Erkrankung der Hirnrinde. Allgemeine Zeitschrift fur Psychiatrie und Psychisch-gerichtliche Medizin, Jan: (1907)

3. Avila J, Lucas J J, Perez M, Hernandez F: Role of tau protein in both physiological and pathological conditions. Physiological Reviews, 84: 361-384 (2004)

4. Bekris L M, Yu C E, Bird T D, Tsuang D W: Genetics of Alzheimer disease. Journal of geriatric psychiatry and neurology, 23: 213-227 (2010)

5. Bertram L, Tanzi R E: Alzheimer's disease: one disorder, too many genes? Human molecular genetics, 13 Spec No 1: R135-41 (2004)

6. Billings L M, Oddo S, Green K N, McGaugh J L, LaFerla F M: Intraneuronal Abeta causes the onset of early Alzheimer's disease-related cognitive deficits in transgenic mice. Neuron, 45: 675-688 (2005)

7. Bird T D: Genetic aspects of Alzheimer disease. Genetics in medicine : official journal of the American College of Medical Genetics, 10: 231-239 (2008)

8. Bolmont T, Clavaguera F, Meyer-Luehmann M, Herzig M C, Radde R, Staufenbiel M, Lewis J, Hutton M, Tolnay M, Jucker M: Induction of tau pathology by intracerebral infusion of amyloid-beta -containing brain extract and by amyloid-beta deposition in APP x Tau transgenic mice. The American journal of pathology, 171: 2012-2020 (2007)

9. Braak E, Braak H, Mandelkow E M: A sequence of cytoskeleton changes related to the formation of neurofibrillary tangles and neuropil threads. Acta Neuropathologica, 87: 554-567 (1994)

10. Braak H, Braak E: Neuropathological stageing of Alzheimer-related changes. Acta Neuropathologica, 82: 239-259 (1991)

11. Braak H, Del Tredici K: The pathological process underlying Alzheimer's disease in individuals under thirty. Acta Neuropathologica, 121: 171-181 (2011)

12. Braak H, Thal D R, Ghebremedhin E, Del Tredici K: Stages of the pathologic process in Alzheimer disease: age categories from 1 to 100 years. Journal of neuropathology and experimental neurology, 70: 960-969 (2011)

13. Braak H, Thal D R, Ghebremedhin E, Del Tredici K: Stages of the pathologic process in Alzheimer disease: age categories from 1 to 100 years. Journal of neuropathology and experimental neurology, 70: 960-969 (2011)

14. Breitner J C, Wyse B W, Anthony J C, Welsh-Bohmer K A, Steffens D C, Norton M C, Tschanz J T, Plassman B L, Meyer M R, Skoog I, Khachaturian A: APOE-epsilon4 count predicts age when prevalence of AD increases, then declines: the Cache County Study. Neurology, 53: 321-331 (1999)

15. Brunkan A L, Goate A M: Presenilin function and gamma-secretase activity. Journal of neurochemistry, 93: 769-792 (2005)

16. Calhoun M E, Wiederhold K H, Abramowski D, Phinney A L, Probst A, Sturchler-Pierrat C, Staufenbiel M, Sommer B, Jucker M: Neuron loss in APP transgenic mice. Nature, 395: 755-756 (1998)

17. Camero S, Benitez M J, Barrantes A, Ayuso J M, Cuadros R, Avila J, Jimenez J S: Tau protein provides DNA with thermodynamic and structural features which are similar to those found in histone-DNA complex. Journal of Alzheimer's disease : JAD, 39: 649-660 (2014)

18. Campion D, Dumanchin C, Hannequin D, Dubois B, Belliard S, Puel M, Thomas-Anterion C, Michon A, Martin C, Charbonnier F, Raux G, Camuzat A, Penet C, Mesnage V, Martinez M, Clerget-Darpoux F, Brice A, Frebourg T: Early-onset autosomal dominant Alzheimer disease: prevalence, genetic heterogeneity, and mutation spectrum. American Journal of Human Genetics, 65: 664-670 (1999)

19. Capetillo-Zarate E, Staufenbiel M, Abramowski D, Haass C, Escher A, Stadelmann C, Yamaguchi H, Wiestler O D, Thal D R: Selective vulnerability of different types of commissural neurons for amyloid beta-protein-induced neurodegeneration in APP23 mice correlates with dendritic tree morphology. Brain : a journal of neurology, 129: 2992-3005 (2006)

20. Capetillo-Zarate E, Staufenbiel M, Abramowski D, Haass C, Escher A, Stadelmann C, Yamaguchi H, Wiestler O D, Thal D R: Selective vulnerability of different types of commissural neurons for amyloid beta-protein-induced neurodegeneration in APP23 mice correlates with dendritic tree morphology. Brain : a journal of neurology, 129: 2992-3005 (2006)

21. Chen J, Kanai Y, Cowan N J, Hirokawa N: Projection domains of MAP2 and tau determine spacings between microtubules in dendrites and axons. Nature, 360: 674-677 (1992)

22. Clavaguera F, Akatsu H, Fraser G, Crowther R A, Frank S, Hench J, Probst A, Winkler D T, Reichwald J, Staufenbiel M, Ghetti B, Goedert M, Tolnay M: Brain homogenates from human tauopathies induce tau inclusions in mouse brain. Proceedings of the National Academy of Sciences of the United States of America, 110: 9535-9540 (2013)

23. Clavaguera F, Bolmont T, Crowther R A, Abramowski D, Frank S, Probst A, Fraser G, Stalder A K, Beibel M, Staufenbiel M, Jucker M, Goedert M, Tolnay M: Transmission and spreading of tauopathy in transgenic mouse brain. Nature cell biology, 11: 909-913 (2009)

24. Cleary J P, Walsh D M, Hofmeister J J, Shankar G M, Kuskowski M A, Selkoe D J, Ashe K H: Natural oligomers of the amyloid-beta protein specifically disrupt cognitive function. Nature neuroscience, 8: 79-84 (2005)

25. Crary J F: Primary age-related tauopathy and the amyloid cascade hypothesis: the exception that proves the rule? Journal of neurology & neuromedicine, 1: 53-57 (2016)

26. De Strooper B, Vassar R, Golde T: The secretases: enzymes with therapeutic potential in Alzheimer disease. Nature reviews.Neurology, 6: 99-107 (2010)

27. Demuro A, Parker I, Stutzmann G E: Calcium signaling and amyloid toxicity in Alzheimer disease. The Journal of biological chemistry, 285: 12463-12468 (2010)

28. Dickson D W: Pick's disease: a modern approach. Brain pathology (Zurich, Switzerland), 8: 339-354 (1998)

29. Double K L, Halliday G M, Kril J J, Harasty J A, Cullen K, Brooks W S, Creasey H, Broe G A: Topography of brain atrophy during normal aging and Alzheimer's disease. Neurobiology of aging, 17: 513-521 (1996)

30. Du H, Guo L, Yan S S: Synaptic mitochondrial pathology in Alzheimer's disease. Antioxidants & redox signaling, 16: 1467-1475 (2012)

31. Duyckaerts C, Braak H, Brion J P, Buee L, Del Tredici K, Goedert M, Halliday G, Neumann M, Spillantini M G, Tolnay M, Uchihara T: PART is part of Alzheimer disease. Acta Neuropathologica, 129: 749-756 (2015)

32. Ebneth A, Godemann R, Stamer K, Illenberger S, Trinczek B, Mandelkow E: Overexpression of tau protein inhibits kinesin-dependent trafficking of vesicles, mitochondria, and endoplasmic reticulum: implications for Alzheimer's disease. The Journal of cell biology, 143: 777-794 (1998)

33. Elder G A, Gama Sosa M A, De Gasperi R: Transgenic mouse models of Alzheimer's disease. The Mount Sinai journal of medicine, New York, 77: 69-81 (2010)

34. Finder V H: Alzheimer's disease: a general introduction and pathomechanism. Journal of Alzheimer's disease : JAD, 22 Suppl 3: 5-19 (2010)

35. Forman M S, Schmidt M L, Kasturi S, Perl D P, Lee V M, Trojanowski J Q: Tau and alpha-synuclein pathology in amygdala of Parkinsonism-dementia complex patients of Guam. The American journal of pathology, 160: 1725-1731 (2002)

36. Fratiglioni L, Ahlbom A, Viitanen M, Winblad B: Risk factors for late-onset Alzheimer's disease: a population-based, case-control study. Annals of Neurology, 33: 258-266 (1993)

37. Games D, Adams D, Alessandrini R, Barbour R, Berthelette P, Blackwell C, Carr T, Clemens J, Donaldson T, Gillespie F: Alzheimer-type neuropathology in transgenic mice overexpressing V717F beta-amyloid precursor protein. Nature, 373: 523-527 (1995)

38. Goedert M, Clavaguera F, Tolnay M: The propagation of prion-like protein inclusions in neurodegenerative diseases. Trends in neurosciences, 33: 317-325 (2010)

39. Gotz J, Chen F, van Dorpe J, Nitsch R M: Formation of neurofibrillary tangles in P301l tau transgenic mice induced by Abeta 42 fibrils. Science (New York, N.Y.), 293: 1491-1495 (2001)

40. Grundke-Iqbal I, Iqbal K, Quinlan M, Tung Y C, Zaidi M S, Wisniewski H M: Microtubule-associated protein tau. A component of Alzheimer paired helical filaments. The Journal of biological chemistry, 261: 6084-6089 (1986)

41. Haass C, Kaether C, Thinakaran G, Sisodia S: Trafficking and proteolytic processing of APP. Cold Spring Harbor perspectives in medicine, 2: a006270 (2012)

42. Hall A M, Roberson E D: Mouse models of Alzheimer's disease. Brain research bulletin, 88: 3-12 (2012)

43. Hanger D P, Anderton B H, Noble W: Tau phosphorylation: the therapeutic challenge for neurodegenerative disease. Trends in molecular medicine, 15: 112-119 (2009)

44. Hardy J A, Higgins G A: Alzheimer's disease: the amyloid cascade hypothesis. Science (New York, N.Y.), 256: 184-185 (1992)

45. Hebert L E, Weuve J, Scherr P A, Evans D A: Alzheimer disease in the United States (2010-2050) estimated using the 2010 census. Neurology, 80: 1778-1783 (2013)

46. Herzig M C, Winkler D T, Burgermeister P, Pfeifer M, Kohler E, Schmidt S D, Danner S, Abramowski D, Sturchler-Pierrat C, Burki K, van Duinen S G, Maat-Schieman M L, Staufenbiel M, Mathews P M, Jucker M: Abeta is targeted to the vasculature in a mouse model of hereditary cerebral hemorrhage with amyloidosis. Nature neuroscience, 7: 954-960 (2004)

47. Hoover B R, Reed M N, Su J, Penrod R D, Kotilinek L A, Grant M K, Pitstick R, Carlson G A, Lanier L M, Yuan L L, Ashe K H, Liao D: Tau mislocalization to dendritic spines mediates synaptic dysfunction independently of neurodegeneration. Neuron, 68: 1067-1081 (2010)

48. Hsiao K, Chapman P, Nilsen S, Eckman C, Harigaya Y, Younkin S, Yang F, Cole G: Correlative memory deficits, Abeta elevation, and amyloid plaques in transgenic mice. Science (New York, N.Y.), 274: 99-102 (1996)

49. Hurtado D E, Molina-Porcel L, Iba M, Aboagye A K, Paul S M, Trojanowski J Q, Lee V M: A{beta} accelerates the spatiotemporal progression of tau pathology and augments tau amyloidosis in an Alzheimer mouse model. The American journal of pathology, 177: 1977-1988 (2010)

50. Hutton M, Lendon C L, Rizzu P, Baker M, Froelich S, Houlden H, Pickering-Brown S, Chakraverty S, Isaacs A, Grover A, Hackett J, Adamson J, Lincoln S, Dickson D, Davies P, Petersen R C, Stevens M, de Graaff E, Wauters E, van Baren J, Hillebrand M, Joosse M, Kwon J M, Nowotny P, Che L K, Norton J, Morris J C, Reed L A, Trojanowski J, Basun H, Lannfelt L, Neystat M, Fahn S, Dark F, Tannenberg T, Dodd P R, Hayward N, Kwok J B, Schofield P R, Andreadis A, Snowden J, Craufurd D, Neary D, Owen F, Oostra B A, Hardy J, Goate A, van Swieten J, Mann D, Lynch T, Heutink P: Association of missense and 5'-splice-site mutations in tau with the inherited dementia FTDP-17. Nature, 393: 702-705 (1998)

51. Hutton M, Lewis J, Dickson D, Yen S H, McGowan E: Analysis of tauopathies with transgenic mice. Trends in molecular medicine, 7: 467-470 (2001)

52. Iba M, Guo J L, McBride J D, Zhang B, Trojanowski J Q, Lee V M: Synthetic tau fibrils mediate transmission of neurofibrillary tangles in a transgenic mouse model of Alzheimer's-like tauopathy. The Journal of neuroscience : the official journal of the Society for Neuroscience, 33: 1024-1037 (2013)

53. Ittner L M, Gotz J: Amyloid-beta and tau--a toxic pas de deux in Alzheimer's disease. Nature reviews.Neuroscience, 12: 65-72 (2011)

54. Jarrett J T, Lansbury P T,Jr: Seeding "one-dimensional crystallization" of amyloid: a pathogenic mechanism in Alzheimer's disease and scrapie? Cell, 73: 1055-1058 (1993)

55. Jellinger K A, Alafuzoff I, Attems J, Beach T G, Cairns N J, Crary J F, Dickson D W, Hof P R, Hyman B T, Jack C R,Jr, Jicha G A, Knopman D S, Kovacs G G, Mackenzie I R, Masliah E, Montine T J, Nelson P T, Schmitt F, Schneider J A, Serrano-Pozo A, Thal D R, Toledo J B, Trojanowski J Q, Troncoso J C, Vonsattel J P, Wisniewski T: PART, a distinct tauopathy, different from classical sporadic Alzheimer disease. Acta Neuropathologica, 129: 757-762 (2015)

56. Kanemaru K, Takio K, Miura R, Titani K, Ihara Y: Fetal-type phosphorylation of the tau in paired helical filaments. Journal of neurochemistry, 58: 1667-1675 (1992)

57. Kang J, Lemaire H G, Unterbeck A, Salbaum J M, Masters C L, Grzeschik K H, Multhaup G, Beyreuther K, Muller-Hill B: The precursor of Alzheimer's disease amyloid A4 protein resembles a cell-surface receptor. Nature, 325: 733-736 (1987)

58. Kivipelto M, Ngandu T, Fratiglioni L, Viitanen M, Kareholt I, Winblad B, Helkala E L, Tuomilehto J, Soininen H, Nissinen A: Obesity and vascular risk factors at midlife and the risk of dementia and Alzheimer disease. Archives of Neurology, 62: 1556-1560 (2005)

59. Kovacs G G: Invited review: Neuropathology of tauopathies: principles and practice. Neuropathology and applied neurobiology, 41: 3-23 (2015)

60. Lamb B T, Sisodia S S, Lawler A M, Slunt H H, Kitt C A, Kearns W G, Pearson P L, Price D L, Gearhart J D: Introduction and expression of the 400 kilobase amyloid precursor protein gene in transgenic mice [corrected. Nature genetics, 5: 22-30 (1993)

61. Lewis J, Dickson D W, Lin W L, Chisholm L, Corral A, Jones G, Yen S H, Sahara N, Skipper L, Yager D, Eckman C, Hardy J, Hutton M, McGowan E: Enhanced neurofibrillary degeneration in transgenic mice expressing mutant tau and APP. Science (New York, N.Y.), 293: 1487-1491 (2001)

62. Liu C, Gotz J: Profiling murine tau with 0N, 1N and 2N isoform-specific antibodies in brain and peripheral organs reveals distinct subcellular localization, with the 1N isoform being enriched in the nucleus. PloS one, 8: e84849 (2013)

63. Liu C C, Kanekiyo T, Xu H, Bu G: Apolipoprotein E and Alzheimer disease: risk, mechanisms and therapy. Nature reviews.Neurology, 9: 106-118 (2013)

64. Masters C L, Simms G, Weinman N A, Multhaup G, McDonald B L, Beyreuther K: Amyloid plaque core protein in Alzheimer disease and Down syndrome. Proceedings of the National Academy of Sciences of the United States of America, 82: 4245-4249 (1985)

65. Oddo S, Billings L, Kesslak J P, Cribbs D H, LaFerla F M: Abeta immunotherapy leads to clearance of early, but not late, hyperphosphorylated tau aggregates via the proteasome. Neuron, 43: 321-332 (2004)

66. Price J L, Davis P B, Morris J C, White D L: The distribution of tangles, plaques and related immunohistochemical markers in healthy aging and Alzheimer's disease. Neurobiology of aging, 12: 295-312 (1991)

67. Rabe S, Reichwald J, Ammaturo D, de Strooper B, Saftig P, Neumann U, Staufenbiel M: The Swedish APP mutation alters the effect of genetically reduced BACE1 expression on the APP processing. Journal of neurochemistry, 119: 231-239 (2011)

68. Reilly J F, Games D, Rydel R E, Freedman S, Schenk D, Young W G, Morrison J H, Bloom F E: Amyloid deposition in the hippocampus and entorhinal cortex:

quantitative analysis of a transgenic mouse model. Proceedings of the National Academy of Sciences of the United States of America, 100: 4837-4842 (2003)

69. Rice H C, Young-Pearse T L, Selkoe D J: Systematic evaluation of candidate ligands regulating ectodomain shedding of amyloid precursor protein. Biochemistry, 52: 3264-3277 (2013)

70. Rijal Upadhaya A, Capetillo-Zarate E, Kosterin I, Abramowski D, Kumar S, Yamaguchi H, Walter J, Fandrich M, Staufenbiel M, Thal D R: Dispersible amyloid beta-protein oligomers, protofibrils, and fibrils represent diffusible but not soluble aggregates: their role in neurodegeneration in amyloid precursor protein (APP) transgenic mice. Neurobiology of aging, 33: 2641-2660 (2012)

71. Roberson E D, Scearce-Levie K, Palop J J, Yan F, Cheng I H, Wu T, Gerstein H, Yu G Q, Mucke L: Reducing endogenous tau ameliorates amyloid beta-induced deficits in an Alzheimer's disease mouse model. Science (New York, N.Y.), 316: 750-754 (2007)

72. Scheuner D, Eckman C, Jensen M, Song X, Citron M, Suzuki N, Bird T D, Hardy J, Hutton M, Kukull W, Larson E, Levy-Lahad E, Viitanen M, Peskind E, Poorkaj P, Schellenberg G, Tanzi R, Wasco W, Lannfelt L, Selkoe D, Younkin S: Secreted amyloid beta-protein similar to that in the senile plaques of Alzheimer's disease is increased in vivo by the presenilin 1 and 2 and APP mutations linked to familial Alzheimer's disease. Nature medicine, 2: 864-870 (1996)

73. Schwab C, Steele J C, McGeer P L: Pyramidal neuron loss is matched by ghost tangle increase in Guam parkinsonism-dementia hippocampus. Acta Neuropathologica, 96: 409-416 (1998)

74. Selkoe D J: Resolving controversies on the path to Alzheimer's therapeutics. Nature medicine, 17: 1060-1065 (2011)

75. Selkoe D J, Hardy J: The amyloid hypothesis of Alzheimer's disease at 25 years. EMBO molecular medicine, 8: 595-608 (2016)

76. Sokolow S, Henkins K M, Bilousova T, Gonzalez B, Vinters H V, Miller C A, Cornwell L, Poon W W, Gylys K H: Pre-synaptic C-terminal truncated tau is released from cortical synapses in Alzheimer's disease. Journal of neurochemistry, 133: 368-379 (2015)

77. Soto C: Unfolding the role of protein misfolding in neurodegenerative diseases. Nature reviews.Neuroscience, 4: 49-60 (2003)

78. Spires-Jones T L, Attems J, Thal D R: Interactions of pathological proteins in neurodegenerative diseases. Acta Neuropathologica, (2017)

79. Spires-Jones T L, Attems J, Thal D R: Interactions of pathological proteins in neurodegenerative diseases. Acta Neuropathologica, (2017)

80. Strittmatter W J, Saunders A M, Schmechel D, Pericak-Vance M, Enghild J, Salvesen G S, Roses A D: Apolipoprotein E: high-avidity binding to beta-amyloid and increased frequency of type 4 allele in late-onset familial Alzheimer disease. Proceedings of the National Academy of Sciences of the United States of America, 90: 1977-1981 (1993)

81. Sturchler-Pierrat C, Abramowski D, Duke M, Wiederhold K H, Mistl C, Rothacher S, Ledermann B, Burki K, Frey P, Paganetti P A, Waridel C, Calhoun M E, Jucker M, Probst A, Staufenbiel M, Sommer B: Two amyloid precursor protein transgenic mouse models with Alzheimer disease-like pathology. Proceedings of the National Academy of Sciences of the United States of America, 94: 13287-13292 (1997)

82. Terry R D, Masliah E, Salmon D P, Butters N, DeTeresa R, Hill R, Hansen L A, Katzman R: Physical basis of cognitive alterations in Alzheimer's disease: synapse loss is the major correlate of cognitive impairment. Annals of Neurology, 30: 572-580 (1991)

83. Thal D R, Capetillo-Zarate E, Del Tredici K, Braak H: The development of amyloid beta protein deposits in the aged brain. Science of aging knowledge environment : SAGE KE, 2006: re1 (2006)

84. Thal D R, Capetillo-Zarate E, Larionov S, Staufenbiel M, Zurbruegg S, Beckmann N: Capillary cerebral amyloid angiopathy is associated with vessel occlusion and cerebral blood flow disturbances. Neurobiology of aging, 30: 1936-1948 (2009)

85. Thal D R, Rub U, Orantes M, Braak H: Phases of A beta-deposition in the human brain and its relevance for the development of AD. Neurology, 58: 1791-1800 (2002)

86. Thal D R, von Arnim C, Griffin W S, Yamaguchi H, Mrak R E, Attems J, Upadhaya A R: Pathology of clinical and preclinical Alzheimer's disease. European archives of psychiatry and clinical neuroscience, 263 Suppl 2: S137-45 (2013)

87. Townsend M, Shankar G M, Mehta T, Walsh D M, Selkoe D J: Effects of secreted oligomers of amyloid beta-protein on hippocampal synaptic plasticity: a potent role for trimers. The Journal of physiology, 572: 477-492 (2006)

88. Umeda T, Maekawa S, Kimura T, Takashima A, Tomiyama T, Mori H: Neurofibrillary tangle formation by introducing wild-type human tau into APP transgenic mice. Acta Neuropathologica, 127: 685-698 (2014)

89. van Eersel J, Stevens C H, Przybyla M, Gladbach A, Stefanoska K, Chan C K, Ong W Y, Hodges J R, Sutherland G T, Kril J J, Abramowski D, Staufenbiel M, Halliday G M, Ittner L M: Early-onset axonal pathology in a novel P301S-Tau transgenic mouse model of frontotemporal lobar degeneration. Neuropathology and applied neurobiology, 41: 906-925 (2015)

90. Vasconcelos B, Stancu I C, Buist A, Bird M, Wang P, Vanoosthuyse A, Van Kolen K, Verheyen A, Kienlen-Campard P, Octave J N, Baatsen P, Moechars D, Dewachter I: Heterotypic seeding of Tau fibrillization by pre-aggregated Abeta provides potent seeds for prion-like seeding and propagation of Tau-pathology in vivo. Acta Neuropathologica, 131: 549-569 (2016)

91. Vassar R: The beta-secretase, BACE: a prime drug target for Alzheimer's disease. Journal of molecular neuroscience : MN, 17: 157-170 (2001)

92. Villemagne V L, Burnham S, Bourgeat P, Brown B, Ellis K A, Salvado O, Szoeke C, Macaulay S L, Martins R, Maruff P, Ames D, Rowe C C, Masters C L, Australian Imaging Biomarkers and Lifestyle (AIBL) Research Group: Amyloid beta deposition, neurodegeneration, and cognitive decline in sporadic Alzheimer's disease: a prospective cohort study. The Lancet.Neurology, 12: 357-367 (2013)

93. Violet M, Delattre L, Tardivel M, Sultan A, Chauderlier A, Caillierez R, Talahari S, Nesslany F, Lefebvre B, Bonnefoy E, Buee L, Galas M C: A major role for Tau in neuronal DNA and RNA protection in vivo under physiological and hyperthermic conditions. Frontiers in cellular neuroscience, 8: 84 (2014)

94. Wang Y, Mandelkow E: Tau in physiology and pathology. Nature reviews.Neuroscience, 17: 5-21 (2016)

95. Wang Y, Mandelkow E: Degradation of tau protein by autophagy and proteasomal pathways. Biochemical Society transactions, 40: 644-652 (2012)

96. Wang Y J, Zhou H D, Zhou X F: Clearance of amyloid-beta in Alzheimer's disease: progress, problems and perspectives. Drug discovery today, 11: 931-938 (2006)

97. Weuve J, Hebert L E, Scherr P A, Evans D A: Deaths in the United States among persons with Alzheimer's disease (2010-2050). Alzheimer's & dementia : the journal of the Alzheimer's Association, 10: e40-6 (2014)

7. Acknowledgement

This page has been removed for data protection reasons.

Curriculum vitae

This page has been removed for data protection reasons.